Pergamon

Geochimica et Cosmochimica Acta, Vol. 60, No. 9, pp. 1497–1514, 1996

0016-7037/96 $15.00 + .00

PII S0016-7037(96)00036-1

Helium and argon isotopes in rocks, minerals, and related groundwaters: A case study in northern Switzerland

I. TOLSTIKHIN,[1,2] B. E. LEHMANN,[3] H. H. LOOSLI,[3] and A. GAUTSCHI[4]

[1]Department of Earth Sciences, Cambridge University, Cambridge, UK
[2]Geological Institute, Kola Science Centre, Apatity, Russia
[3]Physics Institute, University of Bern, Bern, Switzerland
[4]Swiss National Cooperative for the Disposal of Radioactive Waste (NAGRA), Wettingen, Switzerland

(*Received July* 29, 1994; *accepted in revised form January* 22, 1996)

Abstract—To address the problems related to the transfer of helium and argon isotopes from rocks into related aquifers, the concentrations of U, Th, Li, and K and helium and argon isotopes were measured in a sedimentary sequence from Tertiary to Permo-Carboniferous and in crystalline rocks in northern Switzerland. In addition to whole-rock samples, mineral separates have also been investigated. The observed concentrations of ^{3}He, ^{4}He, and ^{40}Ar in rocks, minerals and groundwaters are compared to calculated values which would result from in situ radiogenic production in a closed system.

This comparison shows that the rocks and minerals have almost completely lost radiogenic in situ produced helium. Loss of ^{3}He and ^{4}He has been controlled by different retention capacities of the rock-forming and accessory minerals and fillings. Therefore, measured ^{3}He/^{4}He ratios in these rocks can differ from the calculated production ratios. The deviation is generally less than a factor of 3. However, in certain chemical sediments, e.g., anhydrites, elevated ratios of ^{3}He/^{4}He up to 15×10^{-8}, which is 20 times the production ratio, were observed. It is postulated that ^{3}H, the precursor of ^{3}He, might be chemically bound in such sediments during the 12.3 years half-life of ^{3}H and that the beta decay energy of ^{3}H is too small to liberate ^{3}He.

The calculated closed-system concentrations of helium in groundwater exceed the measured ones by up to three orders of magnitude, implying that the water/rock system has not been a closed system since the time of sedimentation and that movable waters have removed helium to a discharge area and to the atmosphere. Stagnant old waters, however, could contain high concentrations of helium and supply it to younger movable waters. Aquitards with low permeability (Permian shales) appear to be a more important source of helium isotopes than water-bearing rocks (Permian sandstones). High abundances of all parent elements in the shales, almost complete loss of radiogenic helium, and the enhanced production ratio of ^{3}He/^{4}He $= 7.2 \times 10^{-8}$ in these rocks, similar to the ratio observed in the neighbour Permian aquifer, 9.4×10^{-8}, suggest the shale as a major source of helium isotopes for this aquifer and diffusion as a principal process for helium transfer from the stagnant porewaters in shales into the movable waters in sandstones.

Some sedimentary rocks, e.g., Permian sandstones and shales, contain more helium than could have been produced since the time of sedimentation. While Permian sandstones mainly have retained this excess rare gas component, they have released radiogenic helium. The difference in the retention of these two components most probably demonstrates that migration of radiogenic helium from damage tracks along crystal imperfections to grain boundaries is an important process controlling its loss. The abundances of excess ^{3}He and ^{4}He in rocks cannot be predicted by in situ production calculations; studies of rocks and minerals are required.

The average ratio of ^{40}Ar/^{36}Ar = 385 in groundwaters collected from Permian sediments from the Weiach borehole is much higher than that in the aquifers from the crystalline basement below the sediments. Radiogenic ^{40}Ar* in Permian sediments is mainly liberated by diagenetic water-rock interactions. The low contribution of radiogenic ^{40}Ar* in deep aquifers of the crystalline basement and the fact that chlorine concentrations in groundwaters from the basement are also much lower than in the overlaying Permian aquifer eliminates a hypothetical upwards fluid flux.

From this study we envisage intrabasin sources for helium and argon isotopes in groundwaters with mainly lateral migration of waters through sedimentary layers at different rates and diffusion of helium from "slower-velocity" older waters in more stagnant zones (shales) into flow-passes with "higher-velocity" younger waters in sections with higher permeability (sandstones). An external source for noble gases is not required in such a model.

1. INTRODUCTION

Noble gas abundances in terrestrial fluids enable us to study their sources, water-rock interactions, migration, and mixing. Since Savchenko (1935) considered He/Ar ratios in groundwaters as a measure of their age, a substantial dataset has been accumulated. However, debates on the interpretation of excess helium and other noble gases in groundwaters are still going on.

In groundwaters of sedimentary basins an important discrepancy is sometimes observed between high ^{4}He-concentrations, which correspond to old "U-Th-^{4}He ages," even

approaching the sedimentation ages (Ivanov et al., 1978) and concentrations of radioactive nuclides produced in the atmosphere, e.g., ^{39}Ar or ^{14}C, which indicate orders of magnitude younger ages (Andrews et al., 1983; Torgersen and Clarke, 1985). Therefore, it is important to understand the behaviour of noble gases in the rock-water system.

There is no doubt that rocks are the principal sources of the radiogenic nuclides, e.g. ^{4}He and $^{40}Ar^{*}$, in groundwaters. The problem is whether intrabasin sources are generally sufficient or large-scale fluxes supplying these species to sedimentary aquifers are required.

Therefore, two different approaches have been proposed:

1) The first one envisages homogeneous sedimentary water-bearing layers filled by relatively young groundwaters. In this case the time of accumulation of radiogenic species would be short, i.e., similar to the age of these waters. High concentrations could not arise from intrabasin production. Therefore, a large-scale whole-crustal (in some regions even partially mantle) flux is postulated (Torgersen and Clarke, 1985, 1987; Torgersen et al., 1989; Stute et al., 1992). This interpretation predicts large amounts of movable groundwater which would be available for human use.

2) An alternative interpretation envisages an inhomogeneous porosity and hydraulic conductivity of sedimentary and crystalline rocks and a coexistence of almost immovable older waters, preserved in stagnation zones of sedimentary layers or in closed pores of crystalline rocks, and younger waters flowing within high-porosity and high-conductivity pathways. Radiogenic (e.g., helium), and some other (e.g., Cl) species are accumulating in the older waters. Migration of these species from stagnation zones and/or admixture of the older waters increase their concentrations in the younger waters (Ivanov et al., 1978; Kislitsyn et al., 1987; Kamensky et al., 1991; Bottomley and Veizer, 1992; Fabryka-Martin et al., 1991). In such a case, straightforward mass balance considerations predict small ratios between movable "young" and stagnant "old" waters and, hence, significantly lower amounts of available waters.

To resolve this dilemma a comparison of helium isotope abundances in rocks and in related groundwaters is most important. First, radiogenic helium is the only nuclide which is mainly released from rocks. Therefore, the total input of this tracer into groundwaters can be estimated from the parent element abundances and the sedimentation ages. Second, helium is the only element continuously escaping from the Earth's atmosphere; therefore, the background of atmospheric He in air-saturated waters is extremely small. An input of radiogenic helium can therefore be detected even in open reservoirs (Top et al., 1980; Kipfer, 1991) and in rather young hydrological systems (Schlosser et al., 1989; Kamensky et al., 1991; Solomon et al., 1993). Third, helium is an inert element and, therefore, a conservative tracer of terrestrial fluids. Furthermore, abundances of radiogenic $^{40}Ar^{*}$ and $^{4}He/^{40}Ar^{*}$ ratios in rocks and groundwaters bear important additional evidence on the rate of liberation of radiogenic argon and the scale of fluid migration.

In this contribution we present helium and argon isotope abundances and their parent element concentrations (U, Th, K, Li) in sedimentary and crystalline rocks and rock-forming minerals and discuss sources of noble gas isotopes and factors controlling their loss and migration into related aquifers.

2. SAMPLES

2.1. General Requirements

To study sources of noble gases and processes responsible for their accumulation in groundwaters, different kinds of data are required: the lithology and thickness of the aquifers and aquitards, the permeability and porosity of all types of rocks; mineral composition of rocks, concentration of parent elements and noble gas isotopes in the rocks and minerals; factors controlling retention of the gases, as well as their variations within a sedimentary basin; the structure of sedimentary layers; faults and their relationships with the sediments; the tectonic regime and the seismic activity; the ages of the parent rocks (for clastic sediments) and that of sedimentation; and concentrations of species of interest in groundwaters and radiometric ages of aquifers.

There are not too many test sites where such a dataset is available. One of these is the Tertiary-Carboniferous sedimentary basin in northern Switzerland: almost all of the data mentioned above are available for this test site due to careful hydrogeochemical investigations within the NAGRA (Swiss National Cooperative for the Disposal of Radioactive Waste) programme (Pearson et al., 1991). Noble gas abundances in rocks and related minerals, however, were still missing prior to this study.

2.2. Regional Geology and Hydrogeology

The subdivision of geological units in northern Switzerland relies on structural features. The crystalline basement is only exposed in the Black Forest massif on the northern flank of the sedimentary basin (Fig. 1). The Tabular Jura consists of a thin sequence of slightly faulted Mesozoic-Tertiary sedimentary rocks covering the crystalline basement and the Paleozoic troughs. The Folded Jura is characterised by folds and thrust-planes, mainly formed during the late Miocene and Pliocene, with the main detachment in the evaporitic part of the Triassic. In the Molasse Basin, Oligocene and Miocene detrital sediments, with increasing thickness towards the Alps, lay on the Mesozoic and in some places on the Paleozoic cover of the crystalline basement. In this contribution we use the term Molasse Basin for the whole sequence of rocks from the surface to the crystalline basement.

The groundwater flow regime of northern Switzerland is rather complicated. The sedimentary cover contains some important limestone and sandstone aquifers or aquifer groups, which are separated by aquitards consisting of clays, marls, anhydrite, and rock salt. The deep groundwaters of the different aquifer groups show individual hydrochemical and isotopic characteristics, depending on the host rock mineralogy, geographic location with respect to recharge zones, and the underground residence time.

Samples were selected from cores recovered during NAGRA's deep drilling programme in Northern Switzerland between 1982 and 1989 (Thury and Ammann, 1990; Thury et al., 1994). Seven boreholes (Fig. 1) were drilled to depths of 1300–2400 m, penetrating the sedimentary layers and reaching either the crystalline basement or deep layers of the so-called Permo-Carboniferous Through of northern Switzerland. Most samples in this report are from the Weiach borehole (WEI); a few samples from the crystalline basement of Kaisten (KAI) and Schafisheim (SHA) have been selected for comparison.

2.3. The Weiach Borehole

Figure 2 shows the stratigraphic profile of the Weiach borehole together with the locations of rock and water samples.

During the drilling operation deep groundwaters were sampled from two major aquifers in the Muschelkalk and in the Buntsandstein, from two depths in the Permo-Carboniferous Trough and from two depths in the crystalline basement. Samples of clastic and chemical sediments and crystalline rocks were selected for this study from the aquifers, aquitards, and the basement. Table 1 includes all

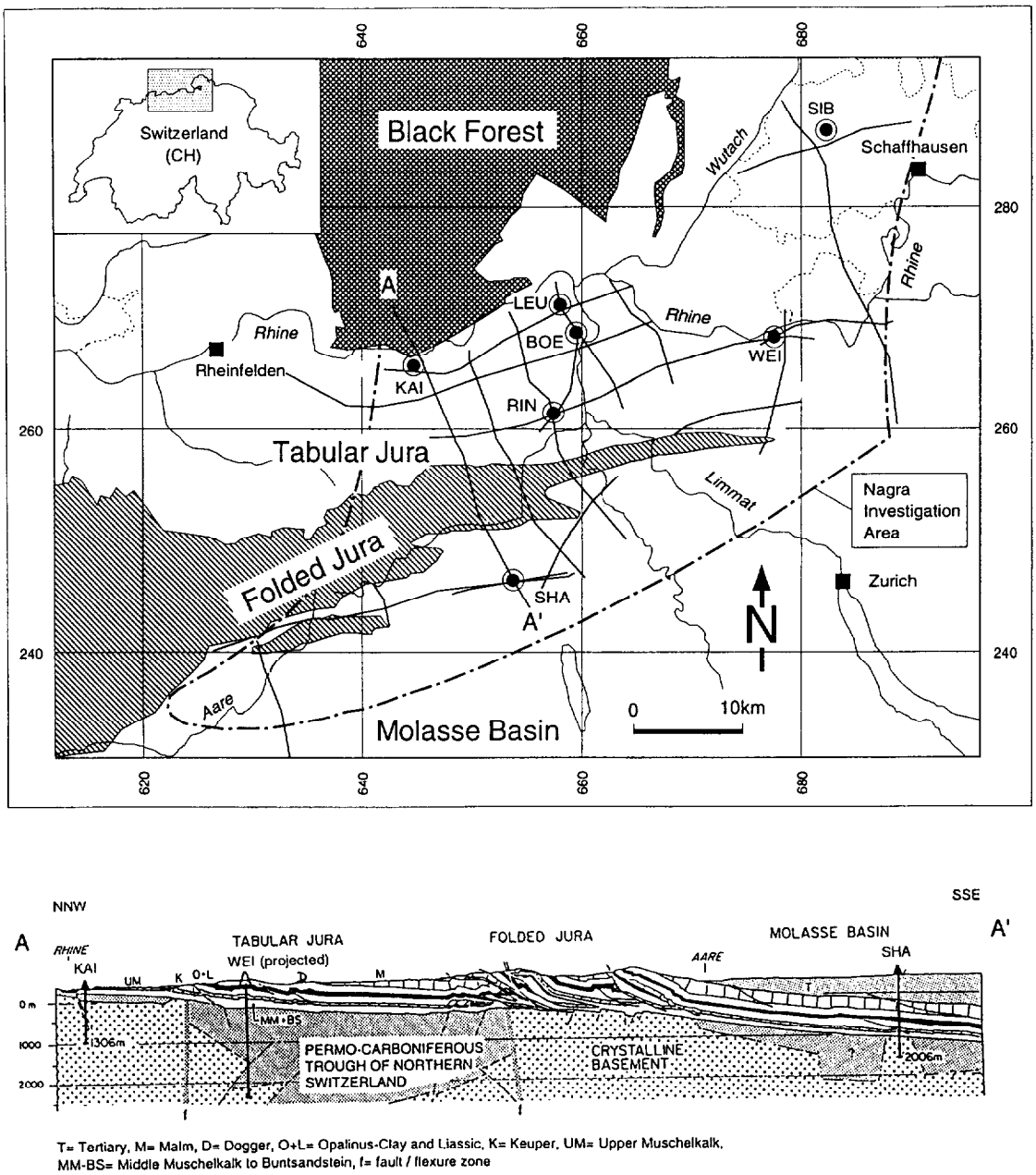

FIG. 1. Geotectonic map of the area and geological cross-section.

samples with reference numbers and a column with the sedimentation age for each stratigraphic unit.

3. EXPERIMENTAL

3.1. Separation of the Rocks and Selection of Minerals

Mineral fractions were separated by heavy liquids, magnetic separation, and HCl treatments (used for sedimentary rocks only). When necessary, minerals were handpicked. Selected minerals were washed in distilled water and dried under temperatures of up to 150°C.

3.2. Extraction System and Mass-Spectrometry

An all-steel system with double-vacuum furnace similar to that described by Staudacher et al. (1978) was used to extract gases and purify the noble gases from chemically active components. Each sample was wrapped into a thin Al foil and mounted on a sample holder, which was then pumped out and some times heated up to 200°C during several days. This preheating did not cause a considerable helium loss from terrigenic sediments (see below and Fig. 5).

Afterwards a sample was dropped into a Mo crucible and heated up to 1700°C for 30 min. Ti-Zr getters purified the noble gases; charcoal traps, cooled by liquid nitrogen, provided separation of helium (with Ne) from argon (and heavier gases). Blanks were measured after five runs using the very same conditions as in the extraction. The total blanks (of the extraction system and the analyser of the mass spectrometer) were 1×10^{-9} and $(30-50) \times 10^{-9}$ cc STP for ^{4}He and ^{40}Ar, respectively. The same extraction system was used for stepwise heating experiments. The duration of each extraction step was one hour.

Crushing of whole-rock samples was carried out under high vac-

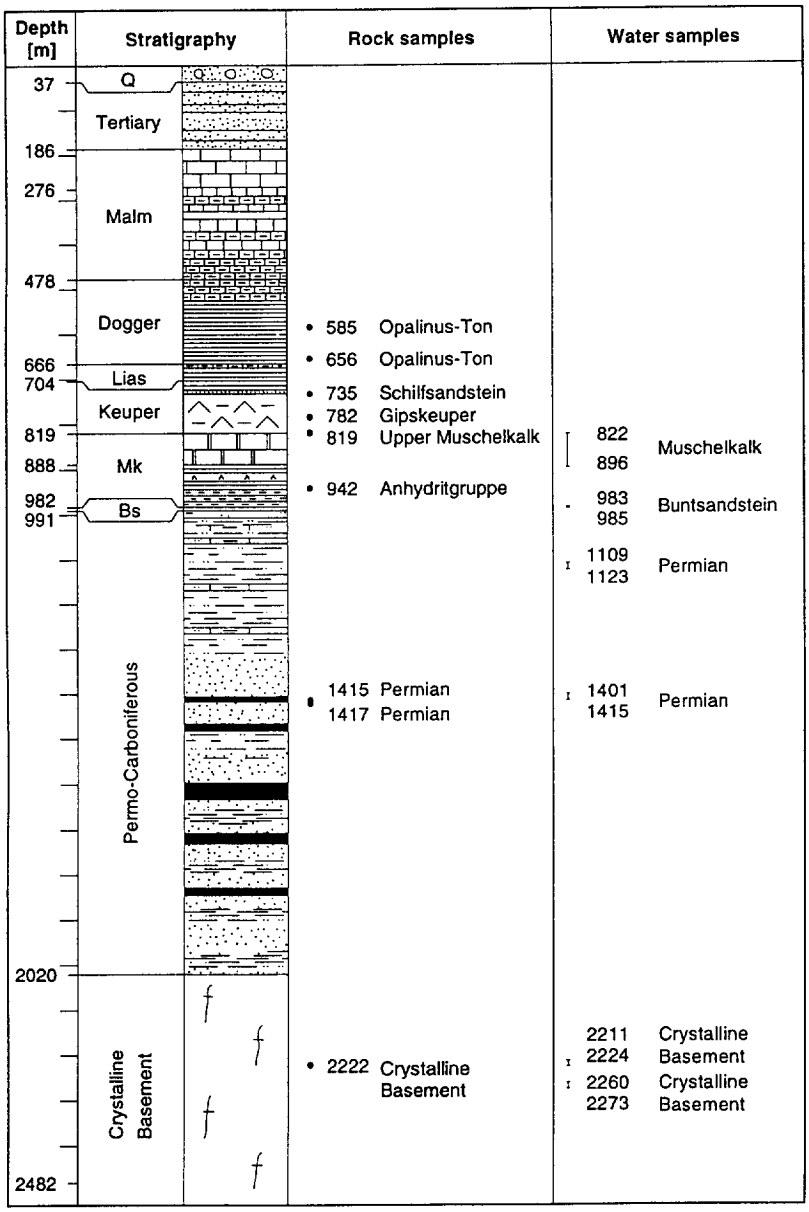

FIG. 2. Stratigraphic profile with depths of boundaries, including selected rock and water samples.

uum in sealed glass ampoules with steel balls inside. Afterwards ampoules were mounted in a vacuum ampoule-holder and opened on by one. Released gases were purified in the system described above and let in the mass spectrometer. Only ^{4}He concentrations and ^{3}He/^{4}He ratios were measured. Helium-4 blanks for the crushing extraction were 1×10^{-8} cc STP/g.

Isotopic compositions and concentrations of helium and argon were measured with a static mass spectrometer MI1201, which provided a complete separation of $^3He^+$ from the hydrogen doublet H_3^+ and HD^+. A high sensitivity for ^{3}He, 5×10^{-5} A/Torr, allowed to measure as low ^{3}He/^{4}He ratios as 1×10^{-8}. The sensitivity for Ar was 3×10^{-4} A/Torr. Standard gases were analysed before and after the measurements to calibrate the mass-spectrometer; the only difference between standard and air gases was the abundance of helium: the ratio of He/Ne in the standard was 200.

Concentrations were measured by the peak height method with an accuracy (1σ is used in this contribution) of $\pm 7\%$. Uncertainties in ^{3}He/^{4}He ratios of $\sim 1 \times 10^{-6}$ and $\sim 3 \times 10^{-8}$ were about $\pm 2\%$ and $\pm 10\%$, respectively. Three repeated ^{3}He/^{4}He measurements, carried out for each of the most interesting samples 1415-SS and 1418-SH, yielded a reproducibility of $\pm 7\%$ for a single measurement of ^{3}He/^{4}He $= 5 \times 10^{-8}$. Uncertainties in ^{40}Ar/^{36}Ar ratios of ~ 300 and $\sim 50{,}000$ were $\pm 0.3\%$ and $\pm 25\%$, respectively.

3.3. Concentrations of U, Th, K, and Li

The concentrations of U and Th were measured by X-radiography. The lowest measurable concentration is about 1 ppm. To control the reproducibility of the analysis, U and Th were measured at least twice for each sample and four times for several samples; the uncertainty for the mean values (Table 2) was $\pm 10\%$. Concentrations of K and Li were determined by disintegration of the samples in acids, dissolution in distilled water, and spectrophotometric measurements; the accuracy of these analyses is $\pm 11\%$ and $\pm 8.5\%$ for K and Li, respectively.

4. RESULTS

The principal approach used in this study is to compare observed abundances of rare gases in rocks, minerals, and

Table 1 : Sample description
(capital letters : whole rock samples; lower case letters : mineral fractions)

Depth (m)	Sample	Age (Ma)	Description
			WEIACH
585.85	585-SS	176	OPALINUS-TON, whole rock, layered sandstone/shale
-	585-SC	-	sandstone without layers, with carbonaceous organic matter
-	585-cm	-	carbonaceous organic matter
-	585-qz	-	quartz
656	656-SH	178	OPALINUS-TON, whole rock, shale
735.16	735-SS	227	SCHILFSANDSTEIN, whole rock, layered sandstone/shale
-	735-sh	-	shale interlayers
-	735-bc	-	biotite and chlorite
-	735-mi	-	microcline
-	735-pl	-	plagioclase
-	735-qz	-	quartz
782.53	782-AS	232	GIPSKEUPER, whole rock, anhydritic shale
-	782-ac	-	anhydrite (+carbonate)
-	782-an	-	anhydrite
819.65	819-DM	234	UPPER MUSCHELKALK, whole rock, dolomite
942.85	942-AN	240	ANHYDRITGRUPPE, whole rock, anhydrite
-	942-AN	-	anhydrite, whole rock
-	942-ml	-	marl
-	942-ma	-	marl + anhydrite (1:1)
1415.1	1415-SS	285	PERMIAN, whole rock, sandstone
-	1415-mi	-	microcline
-	1415-pl	-	plagioclase
-	1415-qz	-	quartz
1417.68	1417-SH	285	PERMIAN, whole rock, shale
-	1417-cm	-	carbonaceous organic matter
-	1417-mc	-	mica
-	1417-fs	-	feldspar
-	1417-qz	-	quartz
2222.24	2222-GN	320	CRYSTALLINE BASEMENT, whole rock, gneiss
-	2222-cq	-	carbonate + quartz (1:1)
-	2222-qz	-	quartz
-	2222-fs	-	feldspar
-	2222-mi	-	microcline
-	2222-cl	-	chlorite
-	2222-bi	-	biotite (60%) + chlorite
			SCHAFISHEIM
1893.3	1893-AP	320	CRYSTALLINE BASEMENT, whole rock, aplite
1895.01	1895-ST	320	CRYSTALLINE BASEMENT, whole rock, syenite
-	1895-ml	-	melanocratic part of hybrid rock
-	1895-fc	-	feldspars (+carbonates)
			KAISTEN
486.87	486-GN	320	CRYSTALLINE BASEMENT, whole rock, gneiss
-	486-qz	-	quartz
-	486-fs	-	feldspar
-	486-mu	-	muscovite (sericite)
-	486-nm	-	non-magnetic fraction

groundwaters with those calculated from concentrations of the parent elements and geochronological data.

Table 2 summarises the concentrations of U, Th, K, Li, ^{4}He, and ^{40}Ar and the ratios of ^{3}He/^{4}He and ^{40}Ar/^{36}Ar measured in rocks and minerals (for sample identification see Table 1). From these data the concentrations of ^{3}He, ^{40}Ar*, and ^{4}He/^{40}Ar* ratios have been derived (last three columns in Table 2), where ^{40}Ar* stands for the nonatmospheric argon.

Table 3 shows the "closed-system" concentrations which are calculated for nucleogenic isotopes assuming that no loss or gain of the parent (Li, U, Th, K) and daughter (^{3}He, ^{4}He, and ^{40}Ar*) species occurred from/into rocks and minerals since the age of their formation or metamorphism. Note, that the closed system assumption is selected for comparison only and that this does not imply that the system was indeed a closed one since the time of sedimentation! ^{4}He is calculated from the decay of U and Th and ^{40}Ar from the decay of ^{40}K, respectively, using the age shown for each sample in Table 1.

The calculation of ^{3}He yield is more complicated. Nucleogenic ^{3}He is produced in ^{6}Li$(n, \alpha)^3$H reaction followed by ^{3}H $\rightarrow$ ^{3}He β-decay. ^{3}He-concentrations are derived from:

$$[^3\mathrm{He}] = F \times \sigma(\mathrm{Li}) \times [^6\mathrm{Li}] \times T, \qquad (1)$$

where F is the neutron flux in a rock with lithium-6 concentration [^{6}Li] and age T and σ (Li) = 960 barn is the cross-section for the reaction. The fluxes of thermal neutrons are calculated for the whole-rock elemental compositions (Matter et al., 1987) and parent element abundances (Table 2), applying the numerical code adapted from Andrews (1985) (Lehmann et al., 1992). Because the mean free path of neutrons is about 50 cm, exceeding mineral sizes by a factor of ~1000, the calculated flux is also used to estimate the ^{3}He production in mineral fractions (Table 3).

Also included in Table 3 are K/Ar ages derived from the measured abundances of K and ^{40}Ar* and the ratios of measured (Table 2) over calculated (Table 3) concentrations

Table 2 : Measured rock and mineral data and derived values

Sample	U ppm	Th ppm	K %	Li ppm	^{4}He cc/g 10^{-6}	^{40}Ar cc/g 10^{-6}	^{3}He/^{4}He 10^{-8}	^{40}Ar/^{36}Ar	^{3}He cc/g 10^{-14}	^{40}Ar* cc/g 10^{-6}	^{4}He/^{40}Ar*
585-SS	1.3	13	1.4	65	15	22	1.6	3100	24	20	0.75
585-SC	<1	9.5	0.71	25	20	17	1.8	3240	36	15	1.3
585-cm			2.6	100							
585-qz			1	14	4	26	3.2	5580	13	25	0.16
656-SH	2.3	15	1.9	170	4.7	38	3.8	4500	18	36	0.13
735-SS	2.5	12	3.5	60	5.4	50	2	7670	11	48	0.11
735-sh	1.5	14	4.6	60	4.1	57	2.8	6060	11	54	0.076
735-bc	4.9	29	1.7	200	20	30	6.4	1350	130	23	0.87
735-mi	1.5	6.5	4.4	15	1	64	<10	7400	<10	61	0.016
735-pl	<1	3.6	0.066	20	1.3	4.3	<16	1020	<21	3.1	0.42
735-qz	<1	3.2	0.022	20	1.5	4.4	<10	1030	<15	3.1	0.48
782-AS	1.7	7.5	1.1	70	1.8	20	5.5	2930	9.9	18	0.10
782-ac	<1	6.4	0.03	0.8	0.16	7.5	<10	3060	<1.6	6.8	.024
782-an			0.023	13	0.19	1.7	15	340	2.9	0.22	0.86
819-DM	<1	1	0.083	6.5	0.42	3.5	7.2	400	3.0	0.91	0.46
942-AN	3.4	17	0.12	20	3.7	2.4	14	880	52	1.6	2.3
942-AN			0.12	20	4	3.1	11	730	44	1.9	2.1
942-mi	1.2	1.2	0.94	51	8	6.8	8.3	2100	69	5.8	1.4
942-ma	1.4	5.5	0.49	40	6.8	8	7.9	1820	54	6.7	1.0
1415-SS	2	8.6	3.2	55	180	52	8	3800	1440	48	3.8
1415-mi	3.8	5.2	11	6.5	14	150	7.4	3630	104	140	0.10
1415-pl	<1	1.5	0.077	15	200	4.5	7.3	430	1460	1.4	143
1415-qz	<1	3.8	0.12	15	160	5.1	9.1	470	1460	1.9	84
1417-SH	12	26	3.2	170	57	53	3.5	3900	200	49	1.2
1417-cm	12	30	3	130	15	41	5.5	1140	83	30	0.50
1417-mc			2.9	360	22	37	6.6	1840	150	31	0.71
1417-fs			6.6	21	22	120	8	3560	180	110	0.20
1417-qz			0.32	27	110	8.1	7.5	1020	830	5.8	19
2222-GN	3.6	21	3.1	42	16	36	3.2	2640	51	32	0.50
2222-cq	<1	2.4	0.91	12	26	47	2.4	2460	62	41	0.63
2222-qz	<1	3.4	0.083	12	9.6	1.2	5	670	48	0.67	1.2
2222-fs	4.2	6.5	3	3.6	4	34	4		16	<34	
2222-mi	1.7	3.5	9.6	5.1	1.3	100	4.5	4760	6	94	0.014
2222-cl	2.7	8.2	0.12	160	2.4	4	5.6	670	13	2.2	1.1
2222-bi	3.4	12	0.76	320	6	17	4.2	980	25	12	0.50
1893-AP	3.5	24	3	45	33	33	2.3	4180	76	31	1.1
1895-ST	10	38	2.4	170	72	45	1.4	5570	100	43	1.7
1895-ml					58	36	2.5	11800	150	35	1.7
1895-fc	3.9	8.6	4.9	31	14	88	1.5	4400	21	82	0.17
486-GN	1.3	15	3.3	200	52	30	0.6	4820	31	28	1.9
486-qz	<1	3.5	0.04	15	5.4	2.7	7.6	1020	41	1.9	2.8
486-fs	1.2	4.7	8.5	46	1.2	150	7.5	6890	9	144	0.008
486-mu	1.1	5.9	7.7	70	3.5	150	<17	7060	<60	140	0.025
486-nm					14	28	2.1	4750	29	26	0.54

of ^{3}He, ^{4}He, and ^{40}Ar*, listed in %. These ratios can be viewed as the apparent retention coefficients, $L(^iN)$, for a respective noble gas isotope ^iN.

Table 4 summarises concentrations of ^{4}He and ratios of ^{3}He/^{4}He in vesicles opened by crushing of whole rock samples in vacuum and Table 5 (see Section 5.3) shows concentrations of ^{4}He and the ^{3}He/^{4}He- and ^{40}Ar/^{36}Ar-ratios measured in water samples from the Weiach, Schafisheim, and Kaisten boreholes (after Pearson et al., 1991).

5. DISCUSSION

5.1. Isotopic Composition of He in Rocks and Minerals: Sources of He

5.1.1. Comparison between measured and calculated concentrations and ratios

In this section we compare the measured and calculated concentrations of ^{3}He and ^{4}He in rocks and minerals. For this comparison the apparent retention coefficients for ^{3}He and ^{4}He defined in Section 4 are plotted in Fig. 3. Fairly distinct relationships between the retention of helium isotopes can be recognised from inspection of Fig. 3, as follows:

(1) Most samples scattered between the two dashed lines show similar ^{3}He and ^{4}He retention coefficients mainly from 1 to 20%; these samples are defined as Group 1.

(2) Sandstone 1415-SS and quartz and plagioclase from this rock contain excess ^{4}He and ^{3}He relative to the calculated concentrations (Section 5.1.2).

(3) Some chemical sediments appear to have higher apparent retention coefficients for ^{3}He than for ^{4}He. This group includes anhydrite rock at 942 m and dolomite at 819 m. Both show ~20 times higher ^{3}He/^{4}He-ratios than those predicted by in-situ production (Section 5.1.4).

The low apparent retention coefficients for sedimentary and crystalline rocks from Group 1 indicate that these samples have lost most of their in situ produced radiogenic helium. A particularly low retention of ^{4}He is typical for shales and chemical sediments: $L(^4\text{He}) = 4\%$ in 656-SH, 2% in 782-AS, ~2% in 819-DM, and 2% in 942-AN. In all crystalline rock samples but one $L(^4\text{He}) \leq 11\%$. Crushing of these samples liberates rather small amounts of helium (Table 4).

Table 3 : Calculations and comparisons

Sample	n-flux n/cm^2 /sec 10^{-5}	^3He cc/g 10^{-14}	^4He cc/g 10^{-6}	$^3He/^4He$ 10^{-8}	$^{40}Ar^*$ cc/g 10^{-6}	K/Ar My	L(^{3}He) %	L(^{4}He) %	L(^{40}Ar) %
585-SS	1.96	160	94	1.7	10	330	15	16	200
585-SC	1.96	62	~59	~1	5.1	480	58	~34	300
585-cm	1.96	250							
585-qz	1.96	35					37		
656-SH	2.08	450	130	3.5	14	420	4	4	260
735-SS	2.33	230	150	1.5	33	320	4.8	4	150
735-sh	2.33	230	130	1.8	43	270	4.8	3	130
735-bc	2.33	760	330	2.3	16	320	17	6	150
735-mi	2.33	57	84	0.68	41	320	<17	1	150
735-pl	2.33	76	~38	~2.0	0.62	900	<27	~3	490
735-qz	2.33	76	~35	~2.2	0.21	2000	<19	~4	1500
782-AS	1.67	190	99	1.9	11	370	5.2	2	170
782-ac	1.67	2.2	~57	~0.04	0.29	2600	<73	~0.3	2400
782-an	1.67	35			0.22	230	8.3		100
819-DM	<0.54	5.9	~21	~0.28	0.80	260	>51	~2	110
942-AN	4.60	150	220	0.68	1.2	310	35	2	130
942-AN	4.60	150			1.2	350	29		150
942-ml	4.60	400	44	9.8	9.4	150	17	18	62
942-ma	4.60	320	80	4.0	4.9	310	17	9	140
1415-SS	1.74	200	140	1.4	38	340	720	130	125
1415-mi	1.74	23	180	0.13	130	290	450	8	110
1415-pl	1.74	53	~30	~1.8	0.92	410	2800	~670	150
1415-qz	1.74	53	~49	~1.1	1.4	360	2800	~330	130
1417-SH	12.8	4600	640	7.2	38	350	4.4	9	130
1417-cm	12.8	3300	670	4.8	36	240	2.5	2	85
1417-mc	12.8	9400			35	250	1.6		89
1417-fs	12.8	550			79	380	33		140
1417-qz	12.8	710			3.8	400	120		150
2222-GN	6.28	610	340	1.8	42	240	8.4	5	76
2222-cq	6.28	170	~42	~4.0	12	890	36	~62	340
2222-qz	6.28	170	~51	~3.3	1.1	190	28	~19	60
2222-fs	6.28	52	230	0.23	41	<260	31	2	
2222-mi	6.28	74	100	0.74	130	230	8.1	1	72
2222-cl	6.28	2300	180	12	1.6	420	0.57	1	140
2222-bi	6.28	4600	250	18	10	350	0.54	2	120
1893-AP	6.74	700	360	1.9	41	240	11	9	75
1895-ST	12.8	5000	750	6.7	33	400	2	10	130
1895-ml	12.8								
1895-fc	12.8	910	230	3.9	67	390	2.3	6.1	120
486-GN	3.18	1500	190	7.9	45	200	2.1	27	63
486-qz	3.18	110	~52	~2.1	0.54		37	~10	350
486-fs	3.18	340	91	3.7	120		2.7	1	120
486-mu	3.18	510	98	5.2	100		<12	4	140
486-nm	3.18								

Note to Table 3: Symbol ~ corresponds to samples with [U]<1 ppm. In these cases the ^{4}He-production is dominated by ^{232}Th decay and the calculated concentration of ^{4}He is based on age, [Th] and [U] = 0.5 ppm. The corresponding errors in [^{4}He] and related values are generally less than ~50%.
K-Ar age is calculated from measured K and ^{40}Ar* (Table 2).

Retention of helium in minerals depends on specific features of the crystalline lattices. Microclines are known to release helium easily (Ashkinadze, 1980). This is also the case for the microclines studied in this contribution; 735-mi and 2222-mi have lost almost all ^{4}He, $L(^4\text{He}) \sim 1\%$ (Table 3). The capacity of quartz to retain helium depends strongly on the quality of its crystalline structure. Amorphous quartz is easily penetrable by helium. In contrast, an extremely low diffusion coefficient of $\sim 10^{-20}$ $cm^2 s^{-1}$ was determined for perfect quartz crystals (see Chapter 8.4 in Mamyrin and Tolstikhin, 1984, and references therein). The apparent retention coefficients for quartzes vary from 4 to 40% (Table 3), with the exception of 1415-qz and 1417-qz (see Section 5.1.2).

Because of the different capacities of minerals to retain ^{3}He and ^{4}He, observed ^{3}He/^{4}He ratios in rocks and minerals can differ from those expected from in situ production generally by a factor of ≤ 3 (Fig. 3). For example, in gneiss 2222-GN Li-rich biotite and chlorite contain less ^{3}He than Li-poor quartz; the former minerals have lost almost all radiogenic ^{3}He, $L(^3\text{He}) = <0.6\%$, whereas in the quartz $L(^3\text{He}) = 28\%$. These factors provide the difference between the observed whole-rock ratio of $^3\text{He}/^4\text{He} = 3.2 \times 10^{-8}$ and the calculated production ratio of 1.8×10^{-8}. Samples 1895-ST and 486-GN obviously have a lower whole-rock retention coefficient for ^{3}He than for ^{4}He as illustrated in Fig. 3. A similar fractionation caused by different loss of helium isotopes from rock-forming and accessory minerals was observed earlier in Rapakiwi and Carnmenellis granites (Gerling et al., 1976; Mamyrin and Tolstikhin, 1984; Martel et al., 1990).

^{3}He/^{4}He ratios in He released from crystalline rocks by

Table 4 Helium released from whole-rock samples by crushing

Sample	^{4}He	^{3}He/^{4}He
	cc STP/g	
	10^{-6}	10^{-8}
942-AN	0.76	11.2
942-AN	0.6	11.6
1415-SS	32	9.2
1417-SH	1.2	9.7
2222-GN	2.4	6.2
1893-AP	2.1	10.1
1895-ST	1.6	9.8
486-GN	1.6	2.2

Footnotes to Table 4 :

Amounts of He released from other whole-rock samples were similar to background (section 3.2) and these results are omitted.
In sandstone 1415-SS :
$^{40}Ar^* = 0.91 \times 10^{-6}$ cc STP/g and $^4He/^{40}Ar^* = 35$

crushing (Table 4) are higher than those shown in Table 2. Amounts of helium released in these experiments are rather small and this He does not influence the balance of helium isotopes in the rocks (with the exception of 1415-SS). These observations can be explained by preferential loss of ^{3}He from micas where Li is concentrated: micas are soft easily disintegrating minerals.

Summarising results for samples from Group 1 (Fig. 3):

(1) In full accord with previous results (e.g., Gerling, 1957; Mamyrin and Tolstikhin, 1984), sedimentary and crystalline rocks from the Molasse Basin have lost most of their in situ generated helium.
(2) The observed and calculated production ^{3}He/^{4}He ratios can differ (generally by a factor of 3 or less) because of varying retention of ^{3}He and ^{4}He in minerals.

5.1.2. Not in situ produced (excess) helium

In sandstone 1415-SS (whole rock) and especially in its rock-forming minerals quartz and plagiclase the apparent retention coefficients for ^{3}He and ^{4}He are greater than 100% (Fig. 3) indicating either loss of their radioactive parents, U and Th, or gain of extra He. ^{3}He/^{4}He ratios in this rock and mineral separates (Fig. 4) are all within the narrow range, 7 to 9 ($\times 10^{-8}$). Gas-liquid inclusions in minerals, vesicles, contain a substantial amount of helium with quite a similar ratio of $^3He/^4He = 9.2 \times 10^{-8}$ (Table 4). Both values are well above the production ratio of 1.4×10^{-8} (Table 3). Therefore, almost all helium observed in the sandstone

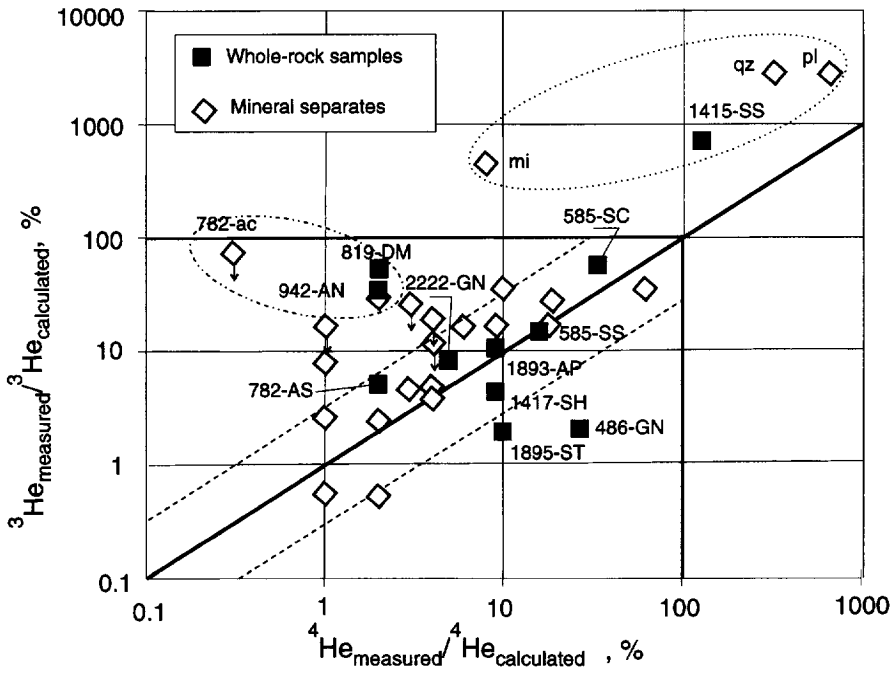

FIG. 3. A comparison of the apparent retention coefficients for ^{3}He and ^{4}He. A majority of data-points with $L(^3He) = L(^4He)$ laying on the thick concordant line and data-points with $L(^3He) \neq L(^4He)$ deviating from this line by a factor of ~3 or less (between the two dashed lines) constitute Group 1 and are discussed in this Section. The apparent retention coefficients for sandstone 1415-SS and its mineral separates (within dotted ellipse) are higher than 100%; these samples are discussed in Section 5.1.2. Some chemical sediments (within dashed-dotted ellipse) show higher retention coefficient for ^{3}He than that for ^{4}He (Section 5.1.4).

should be considered as a component which has not been in situ produced, hereafter refered to as an excess component. In the same rock in situ generated helium has been almost completely lost and its contribution cannot be detected even in microcline 1415-mi with relatively high U, Th, and Li. The contribution of in situ produced helium estimated from stepwise heating extraction is discussed in the next Section 5.1.3.

While sandstone 1415-SS obviously contains excess helium, this can also be the case for some other samples, like for shale 1417-SH. According to the classification presented in Section 5.1.1 (Fig. 3), the shale should belong to Group 1; measured concentrations of both ^{3}He and ^{4}He are well below the calculated ones and the calculated ^{3}He/^{4}He-ratio of 7.2×10^{-8} is only two times higher than the measured ratio of 3.5×10^{-8}. Therefore, at first view helium in this rock seems to be an in situ produced component.

An inspection of the data obtained for minerals, however, leads to quite a different conclusion. Mica 1417-mc with 360 ppm Li should contribute a large portion of ^{3}He to the whole-rock inventory, which is in contrast to what is actually observed. ^{3}He is abundant in quartz 1417-qz with only 27 ppm Li (Table 2). Note that the concentrations of ^{3}He and ^{4}He in 1417-qz are very close to those in 1415-qz (Fig. 4)

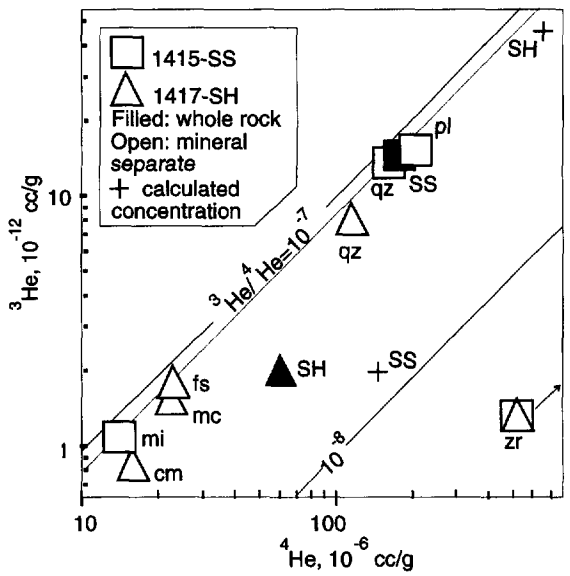

FIG. 4. ^{3}He, ^{4}He concentrations and ^{3}He/^{4}He ratios in sandstone 1415-SS, shale 1417- SH and their mineral separates. The sandstone and its quartz and plagioclase contain excess excess helium with ^{3}He/^{4}He ratio (shown by dotted line) which is ~5 times higher than the production ratio (+SS). Note, microcline from the sandstone and quartz and other mineral separates from the shale show ^{3}He/^{4}He ratios which (1) are almost the same as that in the sandstone (all samples lay close to the dotted line) and (2) do not depend on concentrations of the parent species in the minerals (Table 2). Therefore these minerals probably contain excess He also. High abundances of U, Th, and Li in the shale provide high production of ^{3}He and ^{4}He in this rock (+SH). Carrier of helium with high concentration of ^{4}He = 0.045 cc STP/g and low ^{3}He/^{4}He = $(0.3 \pm 0.1) \times 10^{-8}$ (probably zircon) was found by step wise heating of the sandstone and shale (Section 5.1.3, Fig. 5). This mineral (in the right-bottom corner) allows to obtain a balance of helium isotopes in the shale.

Table 5 Helium and Argon in groundwater samples (After Pearson et al., 1991)

Depth	^{4}He	^{3}He/^{4}He	^{40}Ar/^{36}Ar	Aquifer
m	cc/cc water 10^{-6}	10^{-8}	-	
WEIACH				
859	1.72	13.3	294.4	Muschelkalk (mo)
985	1810	11.2	306.4	Buntsandstein (s)
1116	1590	11.6	395.4	Permian (r)
1408	4480	9.38	375.9	Permian (r)
2218	2580	7.14	296.8	Crystalline (KRI)
2267	2460	-	298.6	Crystalline (KRI)
SCHAFISHEIM				
1571	2740	9.5	310.9	Crystalline (KRI)
1888	910	8.4	348.7	Crystalline (KRI)
KAISTEN				
482	101	20.3	295.8	Crystalline (KRI)
819	99	19.5	297.9	Crystalline (KRI)

which contains excess helium. Moreover, the ^{3}He/^{4}He ratios in the vesicle-related helium from the two rocks are indistinguishable (Table 4). Not only 1417-qz but other minerals separated from shale 1417-SH probably contain excess helium also because ^{3}He/^{4}He ratios in these minerals are almost constant and similar to that in the quartz (Fig. 4).

The potential problem is the source of the excess helium. The ^{3}He/^{36}Ar ratio in the groundwater from the Permian ($\sim 3 \times 10^{-4}$) is comparable to this ratio in sandstone 1415-SS (10.5×10^{-4}). Furthermore, ^{3}He/^{4}He- and ^{4}He/^{40}Ar*-ratios in the groundwater and of excess gases are also similar (see Tables 4, 5, Fig. 8).

Two explanations appear possible. Either there is a common source, such as, e.g., radiogenic species released from shale (Section 5.3.2), or else, helium and argon were trapped before the sedimentation process (Section 5.2.2).

In the later case, the elevated ^{3}He/^{4}He ratios in sandstone 1415-SS could be caused by a small contribution of a mantle fluid to an intracrustal melt. Indications of such processes have been found in several other localities (Kamensky et al., 1990; Tolstikhin et al., 1992; Dunai et al., 1992). Quite similar ratios of ^{3}He/^{4}He $\sim (0.1 - 0.5) \times 10^{-6}$ are typical in fluids from the Black Forest (Griesshaber et al., 1992)-most probable source of detrial sediments in the Molasse Basin (Section 2.2, Fig. 1). Less probably, such a ratio could originate from fractionation of crustal radiogenic helium prior to its being trapped. Fractionation of helium isotopes controlled by their retention in minerals was indeed demonstrated in the Hot Dry Rocks project (Martel et al., 1990): the ^{3}He/^{4}He ratio in a man-made circulated fluid was ~10 times larger than that measured in the host Carnmenellis granite.

It is important to recognise that some rocks and minerals within sedimentary basins can contain excess helium. Abundances of ^{3}He and ^{4}He in these rocks cannot be predicted by in situ production calculations.

5.1.3. *Radiogenic helium in sandstone 1415-SS and shale 1417-SH*

Shale 1415-SH contains less helium than sandstone 1415-SS and the ^{3}He/^{4}He-ratio in shale is lower than in rock-

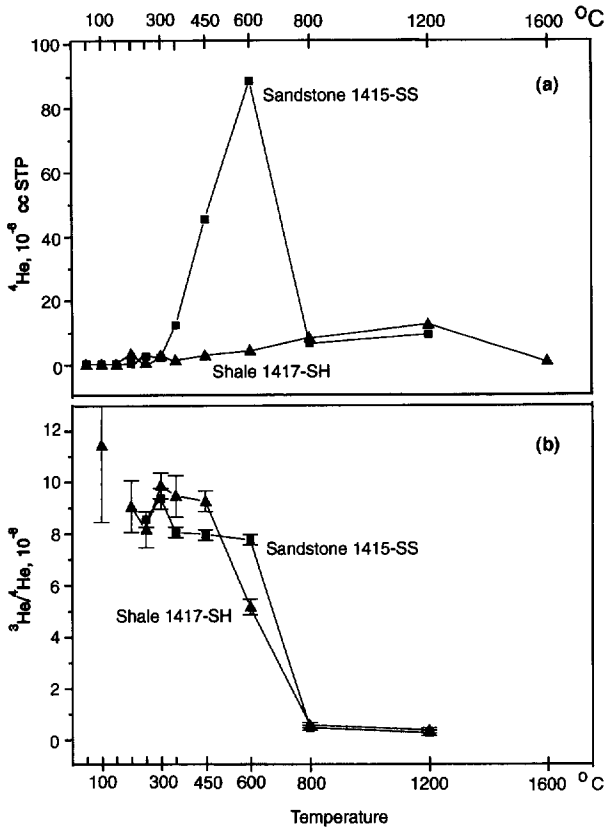

FIG. 5. Stepwise heating release of helium from sandstone 1415-SS and shale 1417-SH. The horizontal axis shows the extraction temperatures. (a) Amounts of ^{4}He released vs. the extraction temperature. The sample weights were 0.9103 and 0.8459 g. The integrated total amounts of ^{4}He released in these experiments were 180×10^{-6} cc STP/g and $40 \cdot 10^{-6}$ cc STP/g for 1415-SS and 1417-SH, respectively. The first concentration is exactly the same as presented in Table 2 and the second one is slightly lower. The concentrations of specific helium with low ^{3}He/^{4}He = 0.4×10^{-8} are $\sim 20 \cdot 10^{-6}$ cc STP per gram of rock or $\sim$0.045 cc STP per gram of zircon, the most probable carrier of such in situ produced helium. (b) ^{3}He/^{4}He ratios in the sandstone and the shale vs. the extraction temperature.

forming minerals and in excess helium (Fig. 4), implying that a mineral fraction with very low ^{3}He/^{4}He ratio was lost probably during mineral separation. To identify this missing ^{4}He-bearing mineral stepwise heating experiments were carried out. The release patterns for the two rocks are quite different (Fig. 5a): a major loss of helium from the sandstone occurs within the temperature interval from 300 to 800°C, while the shale smoothly releases helium within each temperature step from 200 to 1200°C. Both samples, however, contain a noticeable and similar amount of helium which is liberated under relatively high temperatures of 800–1200°C.

In contrast to the release patterns of ^{4}He, the relationships between ^{3}He/^{4}He ratios and extraction temperatures are almost indistinguishable for the two rocks. Elevated ratios of ^{3}He/^{4}He = $(9 \pm 1) \cdot 10^{-8}$ are observed in helium extracted at temperatures lower than 800°C (Fig. 5b). The same ratios are typical of excess He (Fig. 4, Tables 2, 4). Obviously, the excess component is released under the lower temperatures, reinforcing the idea of vesicle-hosted gas.

The combination of high release temperatures, 800–1200°C, low ^{3}He/^{4}He = $(0.2–0.4) \cdot 10^{-8}$, and similar amounts of helium with such ratios in the two samples implies that the carrier of this helium is a retentive U-bearing mineral, which survives sedimentation and diagenetic processes. Zircon appears to be the best candidate. Concentrations of Zr scatter in Permian sediments of the Weiach borehole between 70–330 ppm, without any dependence on concentrations of SiO_2 and Al_2O_3. Therefore, concentrations of zircons in sandstone and shale should be similar. 255 ppm of Zr observed at 1435 m, the depth closest to our samples, corresponds to 440 ppm of zircons, assuming that zircons contain all this Zr. The concentrations of helium with low ^{3}He/^{4}He are $\sim 20 \cdot 10^{-6}$ cc STP per gram of rock (from Fig. 5a) or $\sim$0.045 cc STP per gram of hypothetical zircon. No zircon separates were investigated in this contribution. However, the above concentration seems to be reasonable for 320 Ma zircons with U = 1000 ppm (typical for these minerals). This helium can be classified as the only detectable in-situ produced component. Its ^{4}He concentration is negligibly small relative to the total production; the ratios of measured in stepwise heating ($\sim 20 \cdot 10^{-6}$ cc STP/g) over calculated whole-rock concentrations (Table 3) are 0.14 and 0.03 for the sandstone and the shale, respectively. Most of the in situ produced helium has been lost and only the best bound fraction survived.

An important inference from this study is that minerals of one and the same rock can well retain excess helium but almost completely release radiogenic helium. Different residence times for excess and radiogenic components suggest that migration first along damage tracks (produced by α-particles and tritons) and further along crystal imperfections and grain boundaries is the principal process of liberation of in situ produced helium from minerals.

5.1.4. *^{3}He in chemical sediments*

Dolomite 819-DM, anhydrite 942-AN, and anhydrite fraction 782-an contain small amounts of He with elevated ^{3}He/^{4}He ratios of 7×10^{-8}, 14×10^{-8}, and 15×10^{-8}, respectively, which are by a factor of $\sim$20 above the calculated values. These elevated ratios are noteworthy since release of helium from such rocks/minerals can influence the ratio in groundwaters. It is not possible to attribute the observed ratios to one specific process yet. Several possibilities are discussed below; the last one appears to be more likely than the others.

All these samples were formed in shallow waters (Dronkert et al., 1990), in a continental playa (782-AS), in hypersaline lagoons (gypsum), and in a lagoonal to very shallow marine environment (819-DM). Subsequently, during burial diagenesis at shallow depth, gypsum dehydrated to anhydrite (942-AN). Saturation of these sediments with atmospheric gases is therefore expected. However, high ^{3}He/^{36}Ar ratios in these samples exclude an atmospheric source for ^{3}He.

In samples formed and/or exposed on the Earth's surface, ^{3}He could be yielded by spallation. However, as discussed above, the sediments were most likely formed below a shallow cover of water which effectively shielded the flux of cosmic rays (Lal, 1988). Moreover, during anadiagenesis

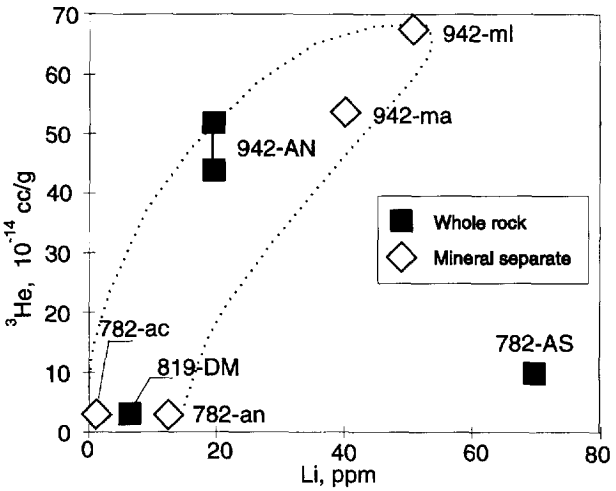

FIG. 6. Relationships between concentrations of ^{3}He and Li in chemical sediments.

accompanied by a massive volume shrink, the gypsum lost its water and a considerable loss of the trapped atmospheric and hypothetical spallogenic He must have occurred during this dehydration process. Therefore, a surface source for ^{3}He in the chemical sediments appears to be unlikely.

Trapping of mantle derived helium after burial of the sediments could potentially elevate the ^{3}He/^{4}He ratio. A stirring up of partially mantle fluid and related heat flow (Polyak and Tolstikhin, 1985) should affect a basin as a whole. However, in the Molasse Basin there are no indications of volcanic, magmatic or hydrothermal activity in the Triassic period and later. Therefore, a deep external source of ^{3}He in the chemical sediments can also be eliminated.

A direct correlation between Li and ^{3}He as presented in Fig. 6 for the chemical sediments would not be expected for any processes mentioned above. Kennedy et al. (1992) also observed enhanced ratios of ^{3}He/^{4}He = 60×10^{-8} unsupported by Li ~120 ppm in anhydrite nodules from the Texas–Oklahoma Hugoton Gas Field. The observed weak relationship between parent Li and daughter ^{3}He point to a radiogenic in situ production of ^{3}He.

Generation of ^{3}He in such minerals as Li-bearing cyclosilicates, e.g., tourmaline or spodumene which are able to retain helium, could cause enhanced ^{3}He/^{4}He in a rock. However, those minerals are not typical for the chemical sediments of the Molasse Basin. The high apparent retention coefficients could result from a higher loss of Li than ^{3}He from rocks (minerals). In this case, to reconcile calculated ^{3}He/^{4}He ratios with observed values we have to postulate a massive, rather late loss of Li: for 942-AN a recent loss of Li by a factor of 20 is required. This translates into an original Li content of ~400 ppm which is a high but still possible concentration (Kennedy et al., 1992 and references therein). Also, chemical and shale minerals with extremely low K (735-qz, 782-ac, Table 3) show unacceptably high apparent K-Ar ages. Rather high ^{40}Ar*/K ratios in these minerals are in accord with (but not necessarily required) a preferential loss of the parent species.

Another explanation of a preferential retention of ^{3}He in the chemical sediments involves quite a different behaviour of H and helium. The parent isotope of ^{3}He is ^{3}H which is produced in the ^{6}Li(n, α)^{3}H-reaction. Both ^{4}He and ^{3}H are emitted with fairly large energies and create damaged tracks in a host mineral. ^{4}He is expected to escape easily along these tracks into crystal imperfections or grain boundaries (Gerling, 1957; Ashkinadze, 1980) where U and Th are usually concentrated. ^{3}H might have quite a different fate. It is most likely that an ion $^3H^+$ immediately attaches to an H_2O molecule to form an H_3O^+ ion which must be much less mobile than a helium atom. Alternatively, ^{3}H could be trapped by chemical sorption or surface solution. By the time ^{3}H decays to ^{3}He (half-life of tritium is 12.3 a), the track could be closed and the ^{3}H-bearing compound effectively trapped. The low energy available in the ^{3}H-decay might not be sufficient to liberate ^{3}He atoms from these recovered tracks. Such a mechanism requires the damaged tracks to have a shorter lifetime in chemical marine sediments than in silicate minerals; annealing of tracks in carbonates and anhydrites at slightly elevated temperatures should proceed on the 10 year scale which is much shorter than that for alpha and fission tracks in silicates under similar conditions.

It is worthwhile to note that Hiyagon and Kennedy (1992) observed elevated ratios of ^{3}He/^{4}He ~$(15-55) \times 10^{-8}$ in methane-bearing gases related to dolomites, anhydrites, and dolomitized rocks, Alberta Canada, and also mentioned that the enhanced ratios were found in fluids related to chemical sediments in some other localities.

More work is needed to understand which process is responsible for elevated ^{3}He/^{4}He ratios in chemical sediments. However, these observations show that in some cases sedimentary rocks contain helium with higher ^{3}He/^{4}He ratios than those predicted by the presently available model. Release of such helium can cause an unexpected ^{3}He anomaly in related groundwaters.

5.2. Radiogenic ^{40}Ar and ^{4}He/^{40}Ar Ratios in Rocks and Minerals

5.2.1. *Argon isotopes*

Radiogenic ^{40}Ar* is known to be retained in minerals much better than helium. The plot of ^{40}Ar/^{36}Ar vs. ^{40}K/^{36}Ar (Fig. 7) is in accord with this general statement: data-points for rocks and minerals cluster around the 320 M.y. reference line, which corresponds to the age of crystallisation or metamorphism of the parent crystalline rocks. The scatter means that either a precursor had not been closed exactly at 320 Ma or, more probably, the rocks/minerals have lost or gained K or ^{40}Ar*. Primary and secondary minerals from one and the same rock indicate redistribution of these species. Even when a whole-rock has lost ^{40}Ar*, some minerals separated from this rock can contain excess ^{40}Ar*. Low concentrations of K are typical of these (probably secondary) minerals. For example, gneiss 2222-GN and K-bearing minerals in this rocks, microcline and feldspar, have lost ^{40}Ar* while carbonate-quartz 2222-cq and chlorite 2222-cl gained ^{40}Ar* so that the K-Ar apparent ages of these minerals (Table 3) are much higher than the accepted age, 320 Ma (Table 1). Sandstone 735-SS lays exactly on the reference 320 Ma isochrone, but

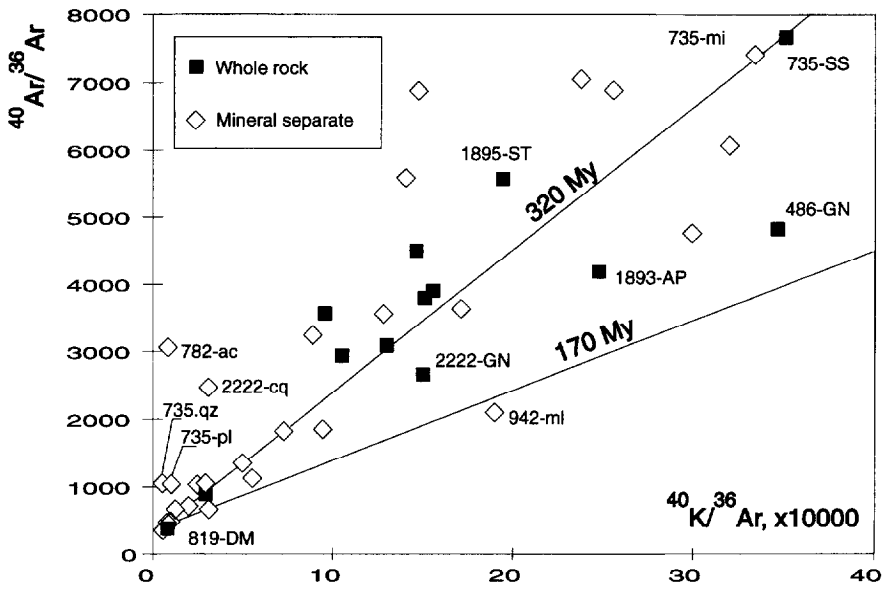

FIG. 7. $^{40}K/^{36}Ar$ – $^{40}Ar/^{36}Ar$ relationship in rocks and mineral. Data-points cluster around the reference 320 M.y. isochrone showing that the release of radiogenic argon from rocks and minerals is not a well-pronounced phenomenon. Secondary minerals (e.g., quartz-carbonate 2222-cq) sometimes contain excess $^{40}Ar^*$ even when the host rock (2222-GN) has lost some $^{40}Ar^*$. Low-K minerals show high apparent K-Ar ages up to 2.6 Ga for anhydrite-carbonate 782-ac.

K-poor plagioclase and quartz from this rock show 3–6 times higher ages (Table 3).

A liberation of $^{40}Ar^*$ from rocks (minerals) can be caused by heating, by opening of fresh fissures due to seismic activity, or by diagenesis, the latter being most probable for the Molasse Sedimentary Basin. A correlation between $^{40}Ar/^{36}Ar$ ratios and K concentrations in groundwaters of the Northern Switzerland (see Fig. 6.5.4 in Pearson et al., 1991) indicates an interaction between the groundwaters and K- and $^{40}Ar^*$-bearing minerals. The dissolution of detrial K-feldspar followed by growth of authigenic K-feldspar, kaolinite, and illite, were observed within specific zones in the Permian sediments (Bluem, 1987). Samples selected for this study do not represent such zones, therefore, quantitative estimates of $^{40}Ar^*$ loss are not possible.

Emphasising the importance of diagenetic processes, it should be mentioned that seismicity could also play a role (Honda et al., 1982; Kislitsyn et al., 1987). For example, the monitoring of $^{40}Ar/^{36}Ar$ ratio in groundwaters, opened by a 1.8 km depth borehole in the Tashkent seismic test site (Uzbekistan, Middle Asia), revealed a postearthquake increasing of $^{40}Ar/^{36}Ar$ from the atmospheric value of 295.5 up to 310 and afterwards decreasing back during ~1 month. The combination of this timescale, the discharge of the borehole, and the porosity of the water-bearing rocks allows to estimate an amount of sedimentary rocks, in which the loss of $^{40}A^*$ had occurred. This amount was found to be rather small, $\sim 10^5$ m^3 (Kislitsyn et al., 1987). This and similar observations reported by Verkhovsky and Shukolyukov (1991) illustrate local sources for radiogenic argon in sedimentary basins.

Summarising, $^{40}Ar^*$ is retained much better than helium and only a small portion is transferred from rocks (minerals) into groundwaters. Loss of $^{40}Ar^*$ occurs within specific local zones; therefore it is difficult to estimate the total input of $^{40}Ar^*$ into groundwaters of a given hydrological system. Regarding the balance of stagnant and movable groundwaters, $^{40}Ar^*$ should be considered as a less promising tracer than helium. However, $^{40}Ar^*$ excess in groundwaters traces specific environments where loss of this nuclide occurs and this enables us to constraint water flow between reservoirs (e.g., Section 5.3.3).

5.2.2. *$^4He/^{40}Ar^*$ in rocks and minerals*

Since rocks and minerals release in situ produced ^4He much easier than $^{40}Ar^*$, the $^4He/^{40}Ar^*$ ratios of species retained in rocks are almost always lower than the production ratio calculated for a given (U + 0.24Th)/K (Fig. 8, see also Mamyrin and Tolstikhin, 1984). A comparison between measured and calculated $^4He/^{40}Ar^*$ ratios in samples from the Molasse Basin confirm this statement (Fig. 8); all measured ratios but one are below the production trend. The measured $^4He/^{40}Ar^*$ ratios in whole-rock samples vary from 0.1 to 1 while the corresponding production ratios are close to 10. The secondary minerals and chemical sediments with low concentrations of K show slightly elevated $^4He/^{40}Ar^*$ ratios compared to the K-bearing micas and microclines.

In groundwaters, which are the complementary reservoir, $^4He/^{40}Ar^*$ ratios generally exceed the production ratios in rocks. Elevated ratios are also typical for trapped fluids (Mamyrin and Tolstikhin, 1984), e.g., for fluids trapped by sandstone 1415-SS and by its minerals, quartz and plagioclase. The ratio measured in gases released from this rock by crushing (i.e., in a trapped fluid) is an order of magnitude higher than the production ratio (Tables 3, 4, Fig. 8). In 1415-qz

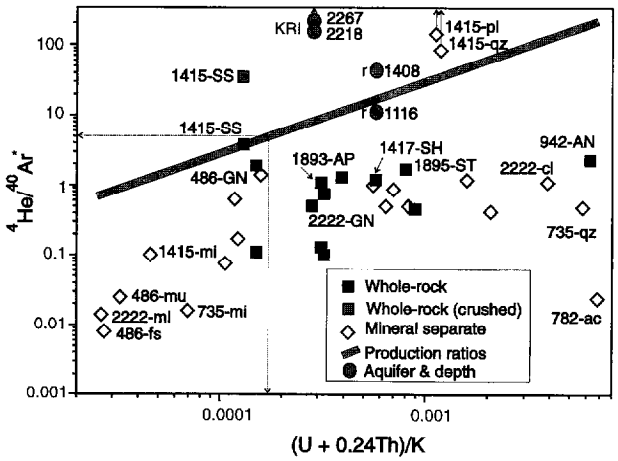

FIG. 8. Relationship between the weighted ratios of parent elements and observed ratios of $^4He/^{40}Ar^*$. The calculated production ratio is shown as straight line for comparison. In (U + 0.24 Th)/K ratio the coefficient 0.24 adjusts for a slower generation of helium from the decay of the Th family (Zartman et al., 1961). The dashed line shows the mean crustal production ratio, 5, corresponding to K/U = 12000 and Th/U = 4. In all samples but one the measured $^4He/^{40}Ar^*$ ratios are lower than the production trend emphasising a preferential loss of radiogenic helium relative to argon. In sandstone 1415-SS which contains excess rare gases the $^4He/^{40}Ar^*$ ratio in gases released by crushing is by a factor of 10 higher than in gases released by melting. Very high $^4He/^{40}Ar^*$ ratios are typical of a fluid trapped by quartz 1415-qz and plagioclase 1415-pl; the ratios corrected for in situ produced $^{40}Ar^*$ in these samples are much higher than the measured ratios. $^4He/^{40}Ar^*$ ratios estimated for Permian aquifers are shown for comparison at the abscissa value for 1417-SH, which is considered as a principal source of radiogenic species in Permian sediments. Ratios for the aquifers from the basement are much higher than the host 2222-GN (should be plotted above the Figure frame).

and 1415-pl, $^4He/^{40}Ar^*$ ratios in gases extracted by melting are even higher, 84 and 143, respectively (Table 2). Moreover, the $^{40}Ar^*$ observed in these minerals includes excess and radiogenic components. The excess $^{40}Ar^*$ can be estimated as a difference between the measured and calculated values from Tables 2 and 3. The measured helium (Table 2) in these minerals was shown to be an excess component (Section 5.1.2). Substitution of these values in

$$(^4He/^{40}Ar^*)_{excess} = {}^4He_{measured}/(^{40}Ar^*_{measured} - {}^{40}Ar^*_{calculated})$$

gives $(^4He/^{40}Ar^*)_{excess}$ ~320 and ~420 for 1415-qz and 1415-pl, respectively. These values are ~100 times the production ratio. Therefore, some specific process had caused severe fractionation of excess noble gases. If the excess gases were trapped by a parent magnetic rock prior to sedimentation then the much higher solubility of helium in silicate melts relative to argon (Hiyagon and Ozima, 1986; Jambon et al., 1986) could be a reason for such a fractionation (Azbel and Tolstikhin, 1988, 1990; Zhang and Zindler, 1989; Spasennykh and Tolstikhin, 1993). Alternatively, if the excess gases originate from a common source (such as, e.g., the shale), then preferential loss of helium and its faster diffusion relative to argon (Jambon and Shelby, 1980; Toyoda and Ozima, 1988; Andrews et al., 1989) might be an explanation for such observations.

5.3. Comparison of Isotope Abundances in Rocks and Related Groundwaters

5.3.1. ^4He-concentrations

The calculated whole-rock concentrations $^4He_{rock}$ (Table 3) and measured porosity values of the rocks (Matter et al., 1987) allow to estimate helium concentrations in the respective water filled pores, $^4He_{water}$, assuming (1) a closed water-rock system since the sedimentation age and (2) that all ^4He produced in the rocks has been transferred into the water:

$$^4He_{water} = {}^4He_{rock} \times ((1 - p)/p) \times (d_r/d_w), \qquad (2)$$

where p, d_r, and d_w are porosity, density of rocks and density of water, respectively. The concentrations (cc STP/g H_2O) calculated for individual rocks range from 2×10^{-4} for 819-DM to $\sim 10^{-1}$ for 2222-GN (open circles in Fig. 9).

The γ-logging measurements of U and Th (Weber et al., 1986) and ~300 measurements of the porosity of Weiach

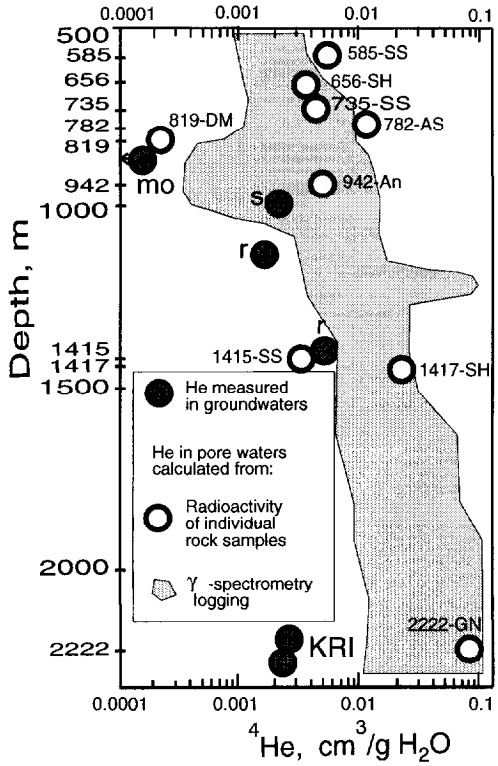

FIG. 9. Measured and calculated concentrations of ^4He in groundwaters vs. depth. Calculated ^4He concentrations in rocks are derived from the concentrations of U and Th (Table 2), the sedimentation ages (Table 1) and the porosity of cores opened by the borehole, assuming the rocks and the waters as a closed system: radiogenic helium released from the rocks and accumulated in groundwater. Data of γ-spectrometry logging are also used for similar estimates. Note, that the calculated closed system concentrations are one or two orders of magnitude higher than those observed in groundwaters, implying that an external source of helium is not required. In the case of Permian aquifers shales rather than water-bearing sandstones are considered as a principle source of radiogenic helium and diffusion as a principal process of helium transfer from stagnant waters in shales to movable waters in sandstones.

cores (Matter et al., 1987) enable us to calculate the closed system concentrations of ^{4}He in groundwaters also: the shadowed area in Fig. 9 represents smoothed results of these calculations.

Three features of the calculated concentrations of ^{4}He in groundwaters can be recognised (Fig. 9):

(1) A general increase of the concentrations with depth, reflecting mainly a decrease of the mean porosity of sediments.

(2) Substantial variations of the concentrations within the 800–1000 m depth interval arising from differences between the chemical and coexisting thin-coarse terrigenic sediments. A high porosity of some chemical sediments and low U and Th contents in these rocks are translated into low calculated concentrations of helium in related groundwaters. Shales are characterised by lower porosity and high U and Th contents and correspondingly by high calculated concentrations of helium.

(3) The concentrations calculated for individual samples (open circles) are within or close to the shadowed field with the exception of 819-DM with the lowest U and Th (Table 2). Such a deviation can occur because the γ-logging averages concentrations of U and Th for a certain depth interval, whereas an individual sample can show an extreme value.

The measured concentrations of ^{4}He in groundwaters (Table 5, closed circles in Fig. 9) cover a great range from 1.7×10^{-6} to 4.5×10^{-3} cc STP/cc water. The lowest measured concentration of ^{4}He in the Upper Muschelkalk groundwater at 859 m corresponds to the lowest calculated concentration (Fig. 9), which arises from a rather high porosity, up to 25%, and low radioactivity, U < 1 ppm, Th = 1 ppm of the Upper Muschelkalk dolomite (sample 819-DM, Table 2). Groundwaters from the Permian formation (depths 1116 and 1408 m), which are probably much older than those from the Upper Muschelkalk (Pearson et al., 1991), show high measured concentrations of ^{4}He. These waters are related to terrigenic sediments with lower porosity, 4–12%, and high radioactivity, U = 2–12 ppm, Th = 8.6–26 ppm (samples 1415-SS, 1417-SH, Table 2). Therefore, the calculated concentrations of ^{4}He are also high (Fig. 9). These relationships between measured and calculated concentrations are expected if ^{4}He is transferred into the groundwaters from neighbouring rocks.

The maximum calculated concentrations of ^{4}He, i.e., the upper boundary of the shadowed area in Fig. 9, are one to three orders of magnitude above the measured concentrations in groundwaters. Therefore, stagnant old waters could contain high amounts of helium and supply this helium to younger movable waters. An external source of ^{4}He is not required for a qualitative interpretation of the data presented in Tables 2, 3, and 5 and in Fig. 9. As a whole, the water-rock system has partially lost in situ produced helium.

Helium could be transferred from stagnant into moveable waters by mixing and/or diffusion. The observed concentrations in groundwaters opened by the Weiach borehole (Table 5, Fig. 9) could result from mixing of a small amount, ~10% or less, of helium-rich waters from aquitards and ~90% of helium-poor waters flowing in aquifers.

Helium could also diffuse from the aquitards, where its concentrations are high, through water-filled pores into the related aquifers with comparatively lower concentrations. A diffusion coefficient for helium in porous rocks of $D = 3 \times 10^{-3}$ m^2 y^{-1} and the mean age of sediments $t = 2 \times 10^8$ years give a rough estimate of the diffusion radius, $r \sim (D \times t)^{1/2} \sim 750$ m. This value is comparable with the thickness of the aquitards in the Weiach borehole (see Fig. 2, also Plate 3 in Pearson et al., 1991). Hence, diffusion appears to be an important process for time and distance scales typical for sedimentary basins (Ivanov et al., 1978).

5.3.2. *^{3}He/^{4}He in rocks, minerals, and groundwaters*

To identify sources of helium further, the measured and calculated ^{3}He/^{4}He ratios in rocks are compared with those measured in groundwaters. Figure 10 summarises all these data for the Weiach borehole (top) and for a few samples from the crystalline basement of Kaisten and Schafisheim boreholes (bottom).

Generally ^{3}He and ^{4}He are released into groundwaters from rocks of a sedimentary basin and/or from external sources. According to the discussion in Section 5.1, the sedimentary rocks of the Molasse Basin could supply related groundwaters with:

1) radiogenic helium with ^{3}He/^{4}He ratios similar to the production ratios;

2) radiogenic helium with ^{3}He/^{4}He ratios which differ from the production ratio up to an order of magnitude, depending on the individual residence times of ^{3}He and ^{4}He in rock-forming minerals, accessory minerals and in fillings; and

3) excess helium with ^{3}He/^{4}He-ratios which can hardly be known without investigations of rocks and minerals; in Permian sandstones of the Molasse Basin the ^{3}He/^{4}He ratio in excess helium exceeds the in situ production ratio.

Very different relations between observed ratios in water and measured and/or calculated ratios in rocks and minerals can result, depending on the importance of the various sources listed above. A discussion of the Weiach borehole from top to bottom illustrates this variety of possible situations (Fig. 10):

1) *Opalinus-Ton (585-SH and 656-SH) and Schilfsandstein* (735-SS)—The measured ^{3}He/^{4}He ratios in rocks and mineral separates are low and close to the calculated in situ production ratio. No groundwater samples have been sampled and analysed.

2) *Gipskeuper (782-AS), Upper Muschelkalk (819-DM) and Anhydritgruppe (942-AN)*—The measured ratios in evaporates and carbonates are significantly higher than the production ratios. The measured ratios in groundwaters (Muschelkalk 859m, Buntsandstein 985m, Table 5) are similar to those measured in rocks or minerals from the same or nearest formations.

3) *Permian sandstone 1415-SS and Shale 1417-SH*—The Permian sediments are mainly composed of sandstones (~50%) and shales (~50%, Fig. 2). Shale 1417-SH has the highest concentrations of U, Th, and Li of all sedimentary rocks from the Weiach borehole (Table 2); therefore, shales are the major source of radiogenic ^{3}He and ^{4}He in Permian rocks. More than 90% of helium produced in the shales

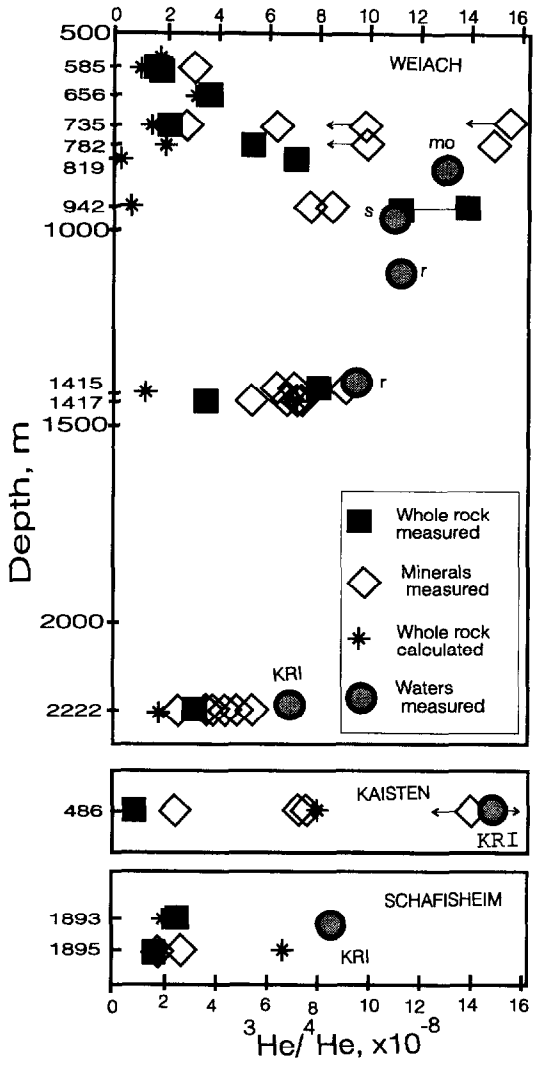

FIG. 10. Measured and calculated $^3He/^4He$ ratios in rocks, minerals, and groundwaters vs. depth. $^3He/^4He$ ratios in groundwaters are close to observed or production ratios in rocks (with the exception of Kaisten, see text). Note, that this ratio in Permian groundwaters (1408 m) is quite similar to the production ratio in adjacent shale 1417-SS. The shale shows high concentrates of U, Th, and Li and produces more helium than any other rock shown in this plot; more than 90% of He has been released in the groundwaters. Water-bearing sandstone 1415-SS contains much less U, Th, and Li then the shale and the production ratio $^3He/^4He$ in this rock is much lower than that observed in the groundwaters. Therefore, shale appears to be the most important source of helium isotopes in Permian sediments. This situation illustrates the importance of aquitards when balance of helium in groundwaters is investigated.

has been transferred into groundwaters. The $^3He/^4He$ ratio observed in Permian groundwaters at 1408 m (9.4×10^{-8}, Table 5) is quite similar to the production ratio in shale 1417-SH (7.2×10^{-8}, Table 3), but substantially higher than the production ratio in water-bearing sandstone 1415-SS (1.4×10^{-8}).

The simplest qualitative interpretation of these data envisages diffusion of helium from the shales into the adjacent Permian aquifer at 1408 m (Table 5); diffusion appears to be the principal process transferring helium from Permian aquitards to aquifers.

4) *Crystalline basement*—The calculated and the measured $^3He/^4He$-ratios in gneiss 2222-GN are both lower than that observed in the groundwater from the crystalline basement of the Weiach borehole (2218 m). Similar relationships are observed for Schafisheim borehole. The maximum $^3He/^4He = 20.3 \times 10^{-8}$ was found in the groundwater from Kaisten (Fig. 10). This borehole is situated on the northwest border of the Molasse Basin close to the Rhein Graben where fluids certainly contain a mantle helium component (Griesshaber et al., 1992). A mixture of mantle He (~2%) and radiogenic helium (~98%) would explain the elevated $^3He/^4He$-ratio of the Kaisten groundwaters. Alternatively but less probably, observed $^3He/^4He$-ratios in groundwaters as high as 20×10^{-8} might be the result of helium isotope fractionation caused by different retention capacity of the various minerals in a rock.

Important issues from Sections 5.3.1 and 5.3.2 are:

1) the helium isotope balance in rocks, minerals, and groundwaters of the Molasse Sedimentary Basin suggest intrabasin sources of helium and

2) the aquitards rather than the aquifers control the balance of helium isotope in groundwaters; diffusion appears to be the mechanism of helium transfer from aquitards to aquifers.

5.3.3. *$^{40}Ar/^{36}Ar$ ratios, water-rock interactions and $^{40}Ar^*$ loss*

Among six deep aquifers opened by the Weiach borehole only the Permian groundwaters contain argon with substantially higher $^{40}Ar/^{36}Ar$ ratios (Table 5) than that in air. A low contribution of $^{40}Ar^*$ in Muschelkalk and waters is most probably a net result of their young age, high porosity of the aquifers, and rather low concentrations of K in chemical sediments which are abundant at these depths (Table 2).

The deep groundwaters from dense crystalline rocks in Weiach, however, also show almost atmospheric $^{40}Ar/^{36}Ar$ ratios and, correspondingly, negligibly small concentrations of $^{40}Ar^*$ which is in contrast to high concentrations of helium in these aquifers.

This contradiction reflects the principal difference in the behaviour of radiogenic helium and argon. In situ produced helium has been almost completely released from any rocks, including crystalline and metamorphic rocks; therefore, the concentrations of helium in groundwaters from the crystalline basement can be high. $^{40}Ar^*$ is liberated in the Molasse Basin mainly by diagenetic processes which are less intense in the basement: opened surfaces required for water-rock interactions are much less available in crystalline rocks than in sediments. Therefore, the high abundance of radiogenic helium implies the old mean age of the groundwaters while the low contribution of $^{40}Ar^*$ shows that these groundwaters were formed in a relatively cold environment with low seismicity and a low ratio between the integrated surface of rocks and the amount of water.

The conclusions form this section are:

1) the low contribution of radiogenic $^{40}Ar^*$ in aquifers from the basement reflects the slow rate of water-rock interaction and

2) $^{40}Ar/^{36}Ar$ ratios in groundwaters from the Weiach borehole eliminate a substantial advection of deep waters from

the basement into Permian aquifers and of Permian waters into the overlaying Muschelkalk aquifer.

5.3.4. $^4He/^{40}Ar^*$ ratios in rocks and groundwaters

For the groundwaters from Permian sediments no reliable measured concentrations of argon are available due to down-hole sampling problems. Therefore, in this section only estimated $^4He/^{40}Ar^*$ ratios in these aquifers are presented. Table 3.3.2 from Pearson et al. (1991) shows that the acceptable measured concentrations are quite similar to the air-saturated concentration of argon in fresh waters at the temperature 10°C, $^{36}Ar = 1.3 \times 10^{-6}$ cc STP/g H_2O (Weiss, 1971). This value, $^{40}Ar/^{36}Ar$ ratios, and ^4He concentrations (Table 5) allow to estimate $^4He/^{40}Ar^*$ ratios in Permian aquifers to be ~12 and ~42 at 1116 and 1408 m, respectively. These ratios are similar to or higher than the production $^4He/^{40}Ar^*$ ratio in shale 1417-SH, the major generator of radiogenic species in Permian sediments (see Fig. 8), and they are reasonably close to those observed in other sedimentary basins (Prasolov, 1990).

A similar approach for the groundwaters from the crystalline basement gives much higher $^4He/^{40}Ar^*$ ratios, ~1500 and ~600 for aquifers at 2218 m and 2267 m, respectively. Because the $^{40}Ar/^{36}Ar$ ratios in waters from the basement (Table 5) are quite close to the atmospheric ratio, the accuracy of these estimates is low and they are valid probably only within a factor of 10. Even taking this into account, the $^4He/^{40}Ar^*$ ratios appears to be much higher than the production and observed ratios in the investigated rocks (Table 2 and 3, Fig. 8), the mean crustal production ratio being 4–5, and those generally observed in terrestrial fluids, 5–25 (Prasolov, 1990).

These results reinforce the conclusions presented in Section 5.3.3; a local specific environment provided a low loss of radiogenic $^{40}Ar^*$.

6. SUMMARY: IMPLICATIONS FOR ISOTOPE HYDROGEOLOGY

Data obtained for sedimentary rocks, minerals, and groundwaters from the Weiach borehole can be qualitatively explained by processes which have occurred within the sedimentary basin.

The inventory of helium isotopes and their parent trace elements in rocks and rock-forming minerals definitely shows that most in situ generated radiogenic helium has been lost from the rocks. Accumulation of this helium in related groundwaters can cause the high concentrations observed in aquifers situated in clastic sediments. The measured helium concentrations in groundwater are lower than the calculated "closed system" values; therefore, the water/rock system as a whole has lost helium since the time of sedimentation.

The role of aquitards appears to be especially important. In the Molasse Basin, Permian shales containing high abundances of the parent elements produce much more ^3He and ^4He than water-bearing sandstones. Moreover, the production ratio of $^3He/^4He$ in the shales is quite similar to that observed in the related Permian aquifer. Because of a low permeability of shales, diffusion of radiogenic nuclides from aquitards to neighbour aquifers appears to be the principal transfer process.

Loss of radiogenic ^3He and ^4He from terrigenic and chemical sediments is accompanied by an isotopic fractionation, caused by a different retention capacity of rock-forming and accessory minerals and fillings. The fractionation could also arise from a specific behaviour of ^3H, the precursor for ^3He. These effects can provide at least a tenfold difference between measured and production $^3He/^4He$ ratio in rocks. When residence times of helium in groundwaters are much shorter than the age of these rocks, this fractionation can affect the $^3He/^4He$ ratio in the groundwaters also. This may be the case for the Muschelkalk aquifer showing low concentration of helium with an elevated $^3He/^4He$ ratio which is quite similar to the ratios observed in related chemical sediments.

Some sedimentary rocks and minerals contain excess helium, whose concentrations, isotopic compositions, and release rates could be quite different from those inferred from the in situ production calculations. In Permian sandstones excess helium is retained much better than helium produced in situ. A substantial difference between retention of excess and radiogenic helium envisages migration of nuclides emitted from parent isotopes through damaged tracks as a process controlling loss of radiogenic helium.

A comparison of groundwaters within the sedimentary basin and those from the crystalline basement suggests intrabasin sources for radiogenic isotopes; a contribution from a hypothetical upwelling fluid is unlikely. The following observations show that groundwaters in the crystalline basement contain less species of interest than those in sedimentary, e.g., Permian, aquifers and therefore cannot be considered as a carrier of these species:

1) $^{40}Ar/^{36}Ar$ ratios in groundwaters from the basement (2218 and 2267 m, Table 5) are lower than those observed in Permian aquifers (1116 and 1408 m). A similar pattern is typical of other boreholes, e.g., Riniken and Kaisten (Fig. 6.5.2 in Pearson et al., 1991), where $^{40}Ar/^{36}Ar$ ratios are lower in groundwaters from the deepest aquifers compared with those from overlaying ones.

2) The total mineralisation and major element chemistry of the highly mineralised Permian groundwaters (Weiach) are quite different from those in the basement. For example, concentrations of Cl up to 1685 meq/L in Permian groundwaters are much higher than ~100 meq/L observed in waters from the crystalline rocks (Tables 1.6.4 and 1.6.5 in Pearson et al., 1991). Similar relationships are found in other boreholes.

The parameters of groundwaters discussed above imply a relatively high permeability of the upper layer of the crystalline basement. According to Thury et al. (1994) and Bottomley and Veizer (1992), the thickness of such a layer could be several hundred meters. Within this layer fractured flow-passes provide a relatively rapid lateral flow, smaller residence times of groundwaters, higher water/rock ratio, lower concentrations of radiogenic nuclides, and lower mineralisation, as compared with these parameters in central segments of a sedimentary basin.

The following studies support the above conclusions. Studies of the Mangyshlak (mainly Jurassic and Cretaceous

sediments, Northern Caspian, Russia), the Northern Usturt (Jurassic-Paleogene) sedimentary basins, the Moscow synclines (Paleozoic), and some other sedimentary basins in Russia did not reveal any considerable contribution of hypothetical helium-bearing fluid from crystalline rocks. In the central segments of the basins diffusion is considered as the principal process. Marginal zones are characterised by higher permeability (Ivanov et al., 1978). The same is probably true for almost all sedimentary basins with the exception of those characterised by extension tectonics, recent magmatism, and/or rather high seismicity.

The hydrology of the oceanic crust is quite different from that on the continents. Nevertheless, data available for ridge-flank sedimentary basins or "ponds" also preclude significant vertical porewater advection from the basement into sedimentary layer, even when the total thickness of sediment cover is as small as ~40 m. In contrast, these data envisage "rapid recharge into, lateral flow through, and discharge out of the basaltic crust" (Baker et al., 1991). Flowmeter measurements indicate the thickness of the highly permeable zone as 330 m (Langeth et al., 1992).

A model which enables us to quantify the helium isotope inventory in sedimentary basins and to estimate the balance of young and old waters should envisage flow channelling within the basin between segments of almost immobile waters. The following processes should be included: mainly lateral migration of waters through sedimentary layers with at least two different speeds; mixing of "slower-velocity" older waters with "higher-velocity" younger ones; and diffusion of helium from stagnant zones into channels with higher permeability.

Acknowledgments—An experimental part of this contribution was partially carried out by our colleagues I. L. Kamensky, V. A. Nivin, and I. V. Tokarev from the Geological Institute, Kola Scientific Centre, Russia; the authors greatly appreciate their assistance. Support of this study by Nagra (Swiss National Cooperative for the Disposal of Radioactive Waste) is gratefully acknowledged. We thank the Swiss National Science Foundation and the Clare Hall and Trinity Colleges for supporting this work in Bern and Cambridge Universities. This work benefited from discussions with Martin Mazurek, Keith O'Nions, David Martel, Bernard Marty, and Friedhelm von Blanckenburg and from review by Mac Kennedy and Robert Poreda. We also thank Balz Kamber, who carefully improved the last version of the manuscript and made many thoughtful comments, and Jane Shears for her kind help with English.

Editorial handling: D. E. Fisher

REFERENCES

Andrews J. N. (1985) The $^3He/^4He$ ratios of radiogenic helium in crustal rocks and its application in groundwater circulation studies. *Chem. Geol.* **49,** 339–351.

Andrews J. N. et al. (1983) *Environmental Isotope Study in Two Aquifer System: A Comparison of Groundwater Dating Methods. Isotope Hydrology; IAEA-SM-270,* pp. 535–576.

Andrews J. N., Hussain N., and Youngman M. J. (1989) Atmospheric and radiogenic gases in groundwaters from the Stripa granite. *Geochim. Cosmochim. Acta* **53,** 1831–1841.

Ashkinadze G. Sh. (1980) *Migration of Radiogenic Isotopes in Minerals.* Leningrad, Nauka.

Azbel I. Ya. and Tolstikhin I. N. (1988) *Radiogenic Isotopes and the Evolution of the Earth's Mantle, Crust and Atmosphere.* Kola Sci. Centre Pub. (in Russian).

Azbel I. Ya. and Tolstikhin I. N. (1990) Geodynamics, magmatism, and degassing of the Earth. *Geochim. Cosmochim. Acta* **54,** 139–154.

Baker P. A., Stout P. M., Kastner M., and Elderfield H. (1991) Large-scale lateral advection of seawater through oceanic crust in the central equatorial Pacific. *Earth Planet. Sci. Lett.* **105,** 522–533.

Bluem W. (1987) Diagenese permischer Schuttfaecher-Sandsteine der Nordschweiz. Eclogae geol. *Helv.* **80/2,** 369–381.

Bottomley D. and Veizer J. (1992) The nature of groundwater flow in fractured rocks: Evidence from the isotopic and chemical evolution of recrystallized fracture calcites from Canadian Precambrian Shield. *Geochim. Cosmochim. Acta* **56,** 369–388.

Dronkert H., Blaesi H.-R., and Matter A. (1990) *Facies and Origin of Triassic Evaporates from the Nagra Boreholes, Northern Switzerland; Nagra Technical Report NTB 87-02.*

Dunai T. J., Touret J. R., and Villa I. M. (1992) Mantle derived helium in fluid inclusions of 2.5 Ga old granulite, Nilgiri Hills, Southern India. In *Water-Rock Interaction* (ed. Y. K. Kharaka and A. S. Maest); *Proc. 7th Int. Symp. on Water-Rock Interaction,* pp. 919–922.

Fabryka-Martin J., Whittemore D. O., Davis S. N., Kubik P. W., and Sharma P. (1991) Geochemistry of halogens in the Milk River aquifer, Alberta, Canada. *Appl. Geochem.* **6,** 447–464.

Gerling E. K. (1957) Migration of helium from rocks and minerals. Trudy Radievigo Instituta. *Acad. Nauk SSSR* **6,** 64–87.

Gerling E. K., Tolstikhin I. N., Drubetskoy E. R., Levkovsky R. Z., Sharkov E. V., and Kozakov I. K. (1976) He and Ar isotopes in rock-forming minerals. *Geochimiya* **11,** 1603–1610 (*Trans. Geochim. Intern.* 1976, 13/6, 1–8).

Griesshaber E., O'nions R. K., and Oxburgh E. R. (1992) Helium and carbon isotopic systematics in crustal fluids from the Eifel, the Rhine Graben and Black Forest, F.R.G. *Chem. Geol.* **99,** 213–235.

Hiyagon H. and Kennedy B. M. (1992) Noble gases in CH_4 gas field, Alberta, Canada. *Geochim. Cosmochim. Acta* **56,** 1569–1589.

Hiyagon H. and Ozima M. (1986) Partitioning of noble gases between olivine and basalt melt. *Geochim. Cosmochim. Acta* **50,** 2045–2057.

Honda M., Kurita K., Hamano Y., and Ozima M. (1982) Experimental studies of He and Ar degassing during rock fracturing. *Earth Planet. Sci. Lett.* **59,** 429–436.

Ivanov V. V., Medovy V. I., and Dobrovolskaya V. I. (1978) Fields of helium concentrations in sedimentary sequences. *Sov. Geol.* **2,** 48–63 (transl. *Intern. Geol. Rev.* **21,** N 8).

Jambon A. and Shelby J. E. (1980) Helium diffusion and solubility in obsidians and basaltic glass in the range 200–300°C. *Earth Planet. Sci. Lett.* **5,** 206–214.

Jambon A., Weber H., and Broun O. (1986) Solubility of He, Ne, Ar, Kr, and Xe in a basalt melt in the range 1250–1600°C. Geochemical implications. *Geochim. Cosmochim. Acta* **50,** 401–408.

Kamensky I. L., Tolstikhin I. N., and Vetrin V. R. (1990) Juvenile helium in ancient rocks: I. ^3He excess in amphiboles from 2.8 Ga charnokite series—Crust-mantle fluid in intracrustal magmatic processes. *Geochim. Cosmochim. Acta* **54,** 3115–3122.

Kamensky I. L., Tokarev I. V., and Tolstikhin I. N. (1991) ^3H-^3He dating: a case for mixing of young and old groundwaters. *Geochim. Cosmochim. Acta* **55,** 2895–2899.

Kennedy B. M., Poths J., and Hiyagon H. (1992) Anomalous ^3He contents in CH_4-rich gases in sedimentary basins. In *Water-rock Interaction* (ed. Y. K. Kharaka and A. S. Maest), pp. 947–950. Balkema.

Kipfer R. (1991) Primordial Edelgase als Tracer fur Fluide aus dem Erdmantel. Zuerich, Dissertation ETH n 9463.

Kislitsyn V. G., Sidikov S., Sultankhodzhaev A. N., Tolstikhin I. N., and Chernov I. G. (1987) Isotopes of argon and helium in rocks, inclusions and waters of Tashkent geodynamic testing area. *Geokhimiya* **8,** 1174–1181.

Lal D. (1988) In situ-produced cosmogenic isotopes in terrestrial rocks. *Ann. Rev. Earth Planet. Sci.* **16,** 355–388.

Langeth M. G., Broecker K., Von Herzen R. P., and Schultheiss P. (1992) Heat and fluid flux trough sediment on the western flank

of the Mid-Atlantic Ridge: A hydrological study of North Pond. *Geophys. Res. Lett.* **19,** 517–520.

Lehmann B. E., Davis S. N., and Fabryka-Martin J. T. (1992) Atmospheric and Subsurface Sources of Stable and Radioactive Nuclides used for Groundwater Dating. *Water Resources Res.* **29,** 2027–2040.

Mamyrin B. A. and Tolstikhin I. N. (1984) *Helium Isotopes in Nature.* Elsevier.

Martel D. J., O'nions R. K., Hilton D. R., and Oxburgh E. R. (1990) The role of element distribution in production and release of radiogenic helium: the Carnmenellis Granite, Southwest England. *Chem. Geol.* **88,** 207–221.

Matter A., Peters T. J., Blaesi H.-R., Meyer J., and Ischi H. (1987) *Sondierbohrung Weiach, Geologie; Nagra Technical Report NTB 86-01* (in German).

Pearson F. J. et al. (1991) *Applied Isotope Hydrogeology-A Case Study in Northern Switzerland; Nagra Technical Report 88-01.*

Polyak B. G. and Tolstikhin I. N. (1985) Isotope composition of earth's helium and the problems of motive forces of tectogenesis. *Chem. Geol.* **52,** 9–33.

Prasolov E. M. (1990) *Isotope Geochemistry and Genesis of Terrestrial Gases.* Nedra (in Russian).

Savchenko V. P. (1935) The problems of geochemistry of helium. *Natural Gases* **9,** 53–197 (in Russian).

Schlosser P., Stute M., Sonntag C., and Munnich K. O. (1989) Tritigenic ^{3}He in shallow groundwater. *Earth Planet. Sci. Lett.* **94,** 245–254.

Solomon D. K., Schiff S. L., Poreda R. J., and Clarke W. B. (1993) A validation of ^{3}H/^{3}He method for determination groundwater recharge. *Water Resources Res.* **29,** 2951–2962.

Spasennykh M. Yu. and Tolstikhin I. N. (1993) Noble gas fractionation during degassing of melts. *Geochim. J.* **27,** 217–221.

Staudacher T., Jessberger E. K., Dorflinger D., and Kiko J. (1978) A refined ultrahigh-vacuum furnace for rare gas. *J. Phys. Sci. Instrum.* **11,** 781–784.

Stute M., Sonntag C., Deak J., and Schlosser P. (1992) Helium in deep circulating groundwater in the Great Hungarian Plain: Flow dynamics and crustal and mantle helium fluxes. *Geochim. Cosmochim. Acta* **56,** 2051–2067.

Thury M. and Ammann M. (1990) *The Seven Nagra Boreholes in Northern Switzerland—Overview of the Investigation Programme; Nagra Bulletin 2/90.* Nagra, Wettingen, Switzerland.

Thury M. et al. (1994) Geology and Hydrogeology of the crystalline basement of Northern Switzerland, Nagra Technical Report NTB 93-01, Nagra, Wettingen, Switzerland, ca. 500p.

Tolstikhin I. N., Dokuchaeva V. S., Kamensky I. L., and Amelin Yu. A. (1992) Juvenile helium in ancient rocks II. U–He, K–Ar, Sm–Nd, and Rb–Sr systematics in the Monche Pluton: ^{3}He/^{4}He ratios frozen in uranium-free ultramafic rocks. *Geochim. Cosmochim. Acta* **56,** 987–999.

Top Z., Clarke W. B., Eismont W. C., and Jones E. P. (1980) Radiogenic helium in Baffin Bay bottom water. *J. Mar. Res.* **38,** 435–452.

Torgersen T. and Clarke W. B. (1985) Helium accumulation in groundwater, I: An evaluation of sources and the continental flux of crustal ^{4}He in the Great Artesian Basin, Australia. *Geochim. Cosmochim. Acta* **49,** 1211–1218.

Torgersen T. and Clarke W. B. (1987) Helium accumulation in groundwater. III: Limits on helium transfer across the mantle-crust boundary beneath Australia and the magnitude of mantle degassing. *Earth Planet. Sci. Lett.* **84,** 345–355.

Torgersen T., Kennedy B. M., Hiyagon H., Chiou K. Y., Reynolds J. H., and Clarke W. B. (1989) Argon accumulation and the crustal degassing flux of ^{40}Ar in the Great Artesian Basin, Australia. *Earth Planet. Sci. Lett.* **92,** 43–56.

Toyoda S. and Ozima M. (1988) Investigation of excess ^{4}He and ^{40}Ar in beryl by laser extraction technique. *Earth Planet. Sci. Lett.* **90,** 69–76.

Verkhovsky A. B. and Shukolyukov Yu. A. (1991) *Element and Isotope Fractionation of Noble Gases in Nature.* Nauka (in Russian).

Weber H. P., Sattel G., and Sprecher C. (1986) *Sondierbohrungen Weiach, Riniken, Schafisheim, Kaisten, Leuggern-Geophysikalische Daten; NAGRA Technical Report NTB-85-50* (in German). NAGRA, Wettingen, Switzerland.

Weiss R. F. (1971) Solubility of helium and neon in water and sea water. *J. Chem. Eng. Data* **16,** 235–241.

Zartman R. E., Wasserburg G. J., and Reynolds J. H. (1961) Helium, argon and carbon in some natural gases. *J. Geophys. Res.* **66,** 277–306.

Zhang Y. and Zindler A. (1989) Noble gas constraints on the evolution of the Earth's atmosphere. *J. Geophys. Res.* **94,** 13,719–13,737.